Biosensors and Bioelectronics 76 (2016) 2–19

Contents lists available at ScienceDirect

Biosensors and Bioelectronics

journal homepage: www.elsevier.com/locate/bios

Aptamer-based nanobiosensors

Yeon Seok Kim [b,1], Nurul Hanun Ahmad Raston [a,1], Man Bock Gu [a,*]

[a] College of Life Sciences and Biotechnology, Korea University, Anam-dong, Seongbuk-gu, Seoul 136-701, South Korea
[b] New Business Division SK Telecom, SK Telecom, 6, Hwangsaeul-ro 258 beon-gil, Bundang-gu, Seongnam, Gyeonggi-do 463-784, South Korea

ARTICLE INFO

Article history:
Received 28 April 2015
Received in revised form
10 June 2015
Accepted 17 June 2015
Available online 20 June 2015

Keywords:
Aptamers
Aptasensors
Nanomaterials

ABSTRACT

It has been more than two decades since aptamer and the systematic evolution of ligands by exponential enrichment (SELEX) method were discovered by Larry Gold and Andrew Ellington in 1990, respectively. Based on the various advantages of aptamers, they have become a potent rival of antibodies in therapeutics and bio-analysis. Especially, the recent advances in aptamer biosensor application are remarkable due to its intrinsic properties of aptamers as nucleic acids and target induced conformational changes, in addition to the introduction of graphene oxide-based easy and simple immobilization-free screening method even for dual aptamers. In addition, the incorporation of various nanomaterials such as metallic nanoparticles, carbon materials, and functional nanospheres in aptasensors has facilitated the improvement of analytical performance and commercial application of aptasensors. In this review, recent prominent reports on aptasensors utilizing nanomaterials were introduced to understand the principle of aptamer-based biosensors and provide an insight for new strategies of aptasensors and the application of various nanomaterials. The perspective on aptamer-based biosensors and diagnostics was also discussed in view of technology and market.

1. Introduction

For four decades, antibodies have dominated the healthcare market based on their effective capturing capacity for proteins. Then, immunoassay has become the most popular platform in clinical tests and biosensors today. Since its first report in 1990, aptamers have received extensive interests as a rival of antibody due to its several advantages compared to antibodies. One of the most important merits of using aptamers is that there are no limitations on their targets. Although antibodies- or enzyme-based assays are well established as a standard biosensor platform for the detection of various targets, they are still restricted in recognizing many of targets, such as toxic small molecules or non-immunogenic targets, and also not easy to recognize the small differences of their macromolecular targets like proteins. To date, thousands of DNA or RNA aptamers have been identified for various targets, such as proteins, peptides, amino acids, antibiotics, small chemicals, viruses, whole or part of cells, and even metal ions, with high affinity and specificity, and they have been applied in various fields, such as diagnostics, therapeutics, biosensors and bio-analytical fields. This fast enrichment of available aptamers should be mainly due to the recent advances in the systematic evolution of ligands by exponential enrichment (SELEX) process, such as the high-throughput and automated SELEX processes, including the most recent development of the immobilization-free screening of aptamers using graphene oxide (Park et al., 2012). According to the advancement on the aptamer screening and development, thousands of articles about aptamers and SELEX have been published, and numerous patents have been issued. Therefore, researchers and companies have obtained more chances to develop or commercialize various platforms of aptasensors for numerous targets, especially since it has been now found that the dual aptamers can be developed cognately (Ahmad Raston and Gu, 2015; Park et al., 2014).

Aptamer-based biosensors among various applications have exceptional merits, compared to the natural receptors, such as antibodies and enzymes. The intrinsic properties of aptamers, as nucleic acids, high flexibility of structure, and convenience in the design of their structure, enable to develop the various novel aptasensors. 1) Aptamers as even complex form with target can be amplified by polymerase chain reaction (PCR). Based on this property, a real-time PCR analysis (Fischer et al., 2008; Lee et al., 2009) and rolling-circle amplification (Cho et al., 2005; Liu et al., 2014b; Yang et al., 2007; Zhou et al., 2007) have been applied in aptasensors for signal amplification. Microarray platform is also available for aptamer-based analysis, in which the quantification of thousands of targets is possible (Kraemer et al., 2011). Besides, any other nucleic detection methods can be adopted for aptasensors by combining both capturing and detection steps. 2) Aptamers fold as

* Corresponding author. Fax: +82 2 928 6050.
E-mail address: mbgu@korea.ac.kr (M. Bock Gu).
[1] Equal contribution.

http://dx.doi.org/10.1016/j.bios.2015.06.040
0956-5663/

Table 1
Nanoparticles applications for aptasensors.

Materials	Target	Assay	Method	LOD	Reference
Gold nanoparticles	Thrombin	Colorimetric	Sandwich	20 nM	(Pavlov et al., 2004)
Gold nanoparticles	Thrombin	Colorimetric	Sandwich (lateral flow strip)	2.5 nM (buffer) 0.6 μM (human plasma)	(Xu et al., 2009a)
Gold nanoparticles	CCRF-CEM	Colorimetric	Sandwich	2 nM	(Medley et al., 2008)
Gold nanoparticles	PDGF	Colorimetric	Sandwich	2.5–10 nM	(Huang et al., 2005)
Gold nanoparticles	PDGFR		Sandwich	3.2 nM	
Gold nanoparticles	PDGF	Colorimetric	TICC[a]	6 nM	(Chang et al., 2013)
Gold nanoparticles	Adenosine	Colorimetric	TID[b]	20 μM (Adenosine) 10 μM (cocaine in buffer) 200 μM (cocaine in blood serum)	(Liu and Lu, 2006)
Gold nanoparticles	Adenosine	Colorimetric	TID	10 μM	(Zhao et al., 2007)
Gold nanoparticles	Adenosine	Colorimetric	TICC	20 μM	(Zhao et al., 2008)
Gold nanoparticles	Hg^{2+}	Colorimetric	TICC	250 nM	(Liu et al., 2008)
Gold nanoparticles	Hg^{2+}	Colorimetric	TID	100 nM	(Ono et al., 2011)
Gold nanoparticles	Pb^{2+}	Colorimetric	TICC	500 nM	(Wei et al., 2008)
Gold nanoparticles	Oxytetracycline	Colorimetric	TICC	25 nM	(Kim et al., 2010b)
Gold nanoparticles	Glutathione	Colorimetric	TID	17 nM (Glutathione) 9 nM (Cysteine) 18 nM (Homocysteine)	(Xu et al., 2012)
Gold nanoparticles	ATP	Colorimetric	TICC	0.6 μM (UV–vis) 2 μM (naked eye)	(Wang et al., 2007)
Gold nanoparticles	Cocaine	Colorimetric	TIA[c]	2 μM	(Zhang et al., 2008b)
Gold nanoparticles	Ibuprofen	Colorimetric	TICC	5 μM	(Kim et al., 2011)
Gold nanoparticles	*Plasmodium vivax* lactate dehydrogenase (PvLDH)	Colorimetric	TICC	10.3 pM (using PDDA) 12.5 pM (using PAH)	(Jeon et al., 2013)
Gold nanoparticles	Theophylline	Fluorometric	TID	0.01–2 mM	(Frauendorf and Jaschke, 2001)
Gold nanoparticles	Hg^{2+}	Fluorometric	TID	5 nM (Hg^{2+}) 300 pM (Pb^{2+})	(Liu et al., 2009a)
Gold nanoparticles	Hg^{2+}	Fluorometric	TICC	0.5 μM	(Kim and Jurng, 2011)
Gold nanoparticles	Ochratoxin A	Fluorometric	TID	5 nM	(Cruz-Aguado and Penner, 2008)
Gold nanoparticles	Pb^{2+} Adenosine	Fluorometric	TID	4 nM 3.4 μM	(Xiang et al., 2009)
Gold nanoparticles	Adenosine	Fluorometric	TID	50 μM (adenosine) 120 μM (cocaine)	(Liu et al., 2007a)
Gold nanoparticles	Adenosine	Fluorometric	TID	2 μM	(Xu et al., 2009b)
Gold nanoparticles	Adenosine	Fluorometric	TID	6 μM (Adenosine) 3 nM (UO_2^{2+}) 8 nM (Pb^{2+}) 30 nM (Hg^{2+})	(Xiang et al., 2010)
Gold nanoparticles	Cocaine	Fluorometric	TID	1 μM	(Xu et al., 2009b)
Gold nanoparticles	Thrombin	Fluorometric	TID	0.14 nM	(Wang et al., 2008)
Gold nanoparticles	Thrombin	Fluorometric	TID	100 nM	(Liu et al., 2014)
Gold nanoparticles	PDGF	Fluorometric	TICC	8 pM (PDGF) 1 nM (PDGF in complex sample) 0.25 nM (thrombin)	(Huang et al., 2007)
Gold nanoparticles	PDGF	Fluorometric	TID	10 pM	(Huang et al., 2008)
Gold nanoparticles	Oxytetracycline	Electrochemical	Simple binding	1–100 nM	(Kim et al., 2009b)
Gold nanoparticles	Thrombin	Electrochemical	Simple binding	2 nM	(Radi et al., 2005)
Gold nanoparticles	Thrombin	Electrochemical	Simple binding	100 pM	(Xu et al., 2006)
Gold nanoparticles	Thrombin	Electrochemical	Sandwich	20 pM	(Li et al., 2008a)
Gold nanoparticles	Cocaine	Electrochemical	TICC	10 μM	(Baker et al., 2006)
Gold nanoparticles	Cocaine	Electrochemical	TICC	0.5 μM	(Li et al., 2008b)
Gold nanoparticles	Cocaine	Electrochemical	TIA	1 μM	(Sharon et al., 2009)
Gold nanoparticles	*Lactobacillus acidophilus*	Electrochemical	TICC	11.0 CFU/ml	(Zuo et al., 2007)
Gold nanoparticles	ATP	Electrochemical	TID TID	0.1 nM (ATP) 0.1 pM (Thrombin)	(Du et al., 2008)
Gold nanoparticles	ATP	Electrochemical	TID	0.1 nM	(Du et al., 2010)
Gold nanoparticles	ATP	Electrochemical	TID	100 nM	(Du et al., 2009)
Gold nanoparticles	Adenosine	Electrochemical	TICC	5 nM	(Wang et al., 2010a)
Gold nanoparticles	VEGF	Electrochemical	Sandwich	30 nM	(Ravalli et al., 2015)
Gold nanoparticles	Mucin 1 protein (MUC1)	Electrochemical	TICC	2.2 nM	(Hu et al., 2014)
Magnetic nanoparticles	Adenosine monophosphate (AMP)	Fluorometric	TIA	0.1 μM	(Song et al., 2009)
Magnetic nanoparticles	Cancer cells	Fluorometric	Simple binding	250 cells	(Smith et al., 2007)
Magnetic nanoparticles	Thrombin	Electrochemical	Sandwich	7.82 aM	(Zheng et al., 2007)
Magnetic nanoparticles	(Carcinoembryonic antigen) CEA	Colorimetric	Catalytic activity	1 ng/ml	(Gao et al., 2008)
Magnetic nanoparticles	DNA	Colorimetric	Catalytic activity	19.4 ± 0.5 ng/μl	(Park et al., 2011)
Magnetic nanoparticles	Hg^{2+}	Colorimetric	TICC	5–75 μM	(Kim and Jurng, 2013)
Gold nanorods	Platelet-derived growth factor AA (PDGF AA)	Fluorometric	Simple binding	10 pM	(Huang et al., 2008)
Gold nanorods	Thrombin	SERS	Sandwich	887 pM	(Wang et al., 2010c)
SWCNTs	Thrombin	FET	Simple binding	10 nM	(So et al., 2005)

well-defined 3-D structure upon binding to target and their conformation are very flexible depending on the existence of target molecules (Cho et al., 2009). 3) The formation of aptamers can be easily modulated using complementary sequences. This aptamer-complementary DNA complex can be easily destroyed by competitive interaction among aptamer, target, and complementary DNA, when the target molecules are added. The design of complementary sequences should be depending on the sequence of aptamer and their affinity with target sophisticatedly. These unique properties of aptamers on the flexible conformational change added a few novel methods in the signal generation on different formats of biosensors, such as simple binding or sandwich-type assay. These approaches are considered to be very powerful especially for the detection of the small molecular targets, since, the sandwich assay format or the mass-dependent detection methods, such as SPR or quartz crystal microbalance (QCM), are not possible due to their small molecular sizes. 4) The easy modification and labeling of dyes or functional group at the end or inter-sites of the aptamer sequence is an another merit to establish the aptamer-based assay format in terms of the signal generation and the well oriented immobilization on solid supports. From these advantages, aptasensors have now been a significantly established in life science, biomedical diagnostics, and biosensors, although they entered only about a decade ago into this bio-analytical field.

In addition, the most recent success in the cognate generation of dual aptamers, which is known to be possible due to the success of aptamer screening without target immobilization, has resulted in opening the use of a sandwich-type sensing platform (Ahmad Raston and Gu, 2015; Park et al., 2014). The advantages of using dual aptamers in aptasensors should be as follow: 1) easy and highly amplified signals can be generated from the use of the secondary signaling aptamer, 2) sandwich-type stable platforms can be definitely adopted, which has been known to be one of the

Table 1 (*continued*)

Materials	Target	Assay	Method	LOD	Reference
SWCNTs	Thrombin	Fluorometric	TID	0.1–1.6 μM	(Zhu et al., 2008)
SWCNTs	Thrombin	NIR	TID	0.1 nM	(Chen et al., 2009a)
SWCNTs	IgE	FET	Simple binding	250 pM	(Maehashi et al., 2007)
SWCNTs	*Salmonella Typhi*	Potentiometric	Simple binding	0.2 CFU/ml 1	(Zelada-Guillen et al., 2009)
SWCNTs	*Escherichia coli*	Potentiometric	Simple binding	6 CFU/ml (in complex matrix) 26 CFU/ml (in apple juice)	(Zelada-Guillen et al., 2010)
SWCNTs	*Staphylococcus aureus*	Potentiometric	Simple binding	8×10^2 CFU/ml	(Zelada-Guillen et al., 2012)
SWCNTs	DNA Antigen	Fluorometric	Sandwich	0.2 pM (DNA) 0.01 nM (Antigen)	(Cui et al., 2008)
Graphene	ATP	Fluorometric	TICC	10 μM	(Wang et al., 2010b)
Graphene	ATP	Fluorometric	TICC	50 nM	(Lu et al., 2010)
Fe_3O_4 graphene oxide	ATP	Electrochemical	TID	0.1 nM	(Tang et al., 2011)
Graphene	ATP	Fluorometric	TID	0.45 μM	(Pu et al., 2012)
Graphene	ATP	Fluorometric	TICC	1.4 μM	(Song et al., 2014)
Graphene	Oxytetracycline	Fluorometric	TICC	10 nM	(Zhao et al., 2013)
Graphene	Lysozyme	Fluorometric	TID	0.08 μg/ml	(Chen et al., 2012a)
Graphene	Cellular prion protein (PrP^C)	Fluorometric	TID	0.309 μg/ml	Zhuang et al., 2013)
Graphene	Lysozyme	SPR	Simple binding	0.5 nM	(Subramanian et al., 2013)
Graphene	Carcino-embryonic antigen	Fluorometric	TICC	5 pg/ml	(Zhou et al., 2014)
Graphene	K^+ Pb^{2+}	Electrochemical	TICC	27 μM (K^+) 2 μM (Pb^{2+})	(Xu et al., 2014)
Graphene	ATP	Fluorometric	TICC	0.019 mM	(Liu et al., 2014c)
Graphene	ATP	Fluorometric	TICC	0.5 μM	(Yi et al., 2014)
Graphene	Thrombin	SPR Electrochemical	TICC	0.05 nM (SPR) 0.03 nM (Electrochemical)	(Wang et al., 2011b)
Graphene	Thrombin	Fluorometric	TICC/TID	10 pM (Thrombin) 60 nM (ATP) 0.8 pM (DNA)	(Liu et al., 2014b)
Graphene/QD composite	Thrombin	Electrochemical	TID	100 nM	(Zhao et al., 2011)
Graphene	PDGF Thrombin	Electrochemical	Sandwich	8 pM (PDGF) 11 pM (Thrombin)	(Bai et al., 2012)
Graphene	Thrombin	Fluorometric	TID	1 nM	(Ueno et al., 2013)
Fe_3O_4 graphene oxide	Prostate specific antigen (PSA)	Fluorometric	TICC	0.5 ng/ml	(Choi and Lee, 2013)
Graphene	Hg^{2+}	Fluorometric	TICC	0.92 nM	(Li et al., 2013)
Silica nanoparticles	Thrombin	Fluorometric	TID and sandwich	1.06 nM	(Wang and Liu, 2009)
Silica nanoparticles	Thrombin	Fluorometric	TISS	4 nM	(Babu et al., 2013)
Silica nanoparticles	ATP	Fluorometric	TIA	20 μM	(Cai et al., 2011)
Quantum dots	Thrombin	Electrochemical	Sandwich	0.55 fM	(Ding et al., 2010a)
Quantum dots	Thrombin	Fluorometric	Simple binding	1 nM	(Chi et al., 2011)
Quantum dots	Cocaine Adenosine	Fluorometric and colorimetric	TIA	120 μM (Cocaine) 50 μM (Adenosine)	(Liu et al., 2007b)
Quantum dots	Cocaine	Fluorometric	TIA	0.5 μM	(Zhang and Johnson, 2009)
Quantum dots	Hg^{2+} K^+ Adenosine	Fluorometric	TICC	0.5 μM (Hg^{2+}) 100 μM (K^+) 5 μM (Adenosine)	(Kim and Jurng, 2011)

[a] TICC target-induced conformation change of aptamer.
[b] TID target-induced displacement of aptamer/DNA probe.
[c] TIA target-induced assembly of aptamer fragments.

weak points using an aptamer, and 3) the realization of aptasensors in markets are now very close, since stripe-type sandwich platform can be used like ELISA or any other antibody-based sandwich assays.

Recently, nanotechnology has added a prominent value to the analytical and diagnostics field, *i.e.* the conjugation of aptamers on various nanomaterials, which has led to highly sensitive and selective aptasensors. The unique properties of nanomaterials such as size- and shape-dependent optical property, easy tuning of surface properties, and catalytic activities are very useful not only for the signal generation but also for the signal amplification. During past few years, there have been great advances in the synthesis of numerous nanomaterials, such as metallic nanoparticles, quantum dots, silica nanoparticles, and carbon nanotubes (Burda et al., 2005), and their application into nanosensors (Baron et al., 2007; Lu and Liu, 2007; Stewart et al., 2008; Wang and Lu, 2009). The integration of aptamers and nanomaterials has been studied actively to develop novel and sensitive sensing system (Lin et al., 2009; Wang et al., 2009a). Although aptasensors are still in its infancy, compared to immunoassay and enzyme-based biosensors, aptamer-based biosensors will be eventually become a great tool by the combination with nanomaterials.

This review summarized recent prominent reports on aptasensors utilizing nanomaterials to understand the principle of aptamer-based biosensors and provide an insight for new design of aptasensing techniques. The perspective on aptasensors was also discussed in view of technology and market.

2. Aptamer-based biosensors using nanoparticles

2.1. Metallic nanoparticles-based aptasensors

2.1.1. Gold nanoparticles

Gold nanoparticles (AuNPs) are considered as the most favorite nanomaterials for the aptasensor development due to their physical and chemical properties. In addition, the conjugation of aptamers on AuNPs by chemisorption or physical adsorption has been well accomplished (Huang et al., 2005; Li and Rothberg, 2004a; Li and Rothberg, 2004b; Mirkin et al., 1996; Pavlov et al., 2004). These features of AuNPs have contributed to conduct simple, efficient and sensitive aptamer-based biosensors. In this section, state-of-the-arts of AuNPs' applications in aptasensors were introduced to give a comprehensive understanding about the strategies for AuNP-based aptasensors and get some clues for creating novel aptasensors. The details on nanoparticles-based aptasensors discussed in this review were summarized in Table 1.

2.2. Colorimetric sensing

The colorimetric detection is a very attractive approach due to its simplicity and low cost for sensing, especially suitable for point-of-care test (POCT). Since the first report of colorimetric DNA detection using AuNPs by Mirkin's group, AuNPs have been most commonly used to develop the colorimetric biosensors based on their unique optical properties, strong localized surface plasmon resonance (LSPR) and high extinction coefficient at the visible wavelength (Mirkin et al., 1996). LSPR quite depends on the interparticle distance of AuNPs, as well as size- and shape of AuNPs (Zhang et al., 2008a). AuNPs with approximately 13 nm in diameter have a maximum SPR absorbance at 520 nm wavelength in dispersion state (observed as red by naked eye), and then shifted to 650 nm, (showing purple color) once aggregated.

AuNPs-based colorimetric aptasensors were summarized into three formats. The first format is a direct observation of localized AuNPs in solution or solid support. The targets are captured by the aptamers immobilised on a solid support like cellulose membrane and the detection of the target can be observed by the secondary aptamer–AuNPs conjugates binding to the targets in a sandwich manner. This method can be easily applied to the conventional sensing platform, but is limited due to the fact that many of identified aptamers are not available for sandwich-type assays, except few of cells and some proteins such as thrombin. Tan's group reported AuNPs-based aptasensors for cancer cell detection, the CCRF-CEM (human acute lymphoblastic leukemia), using aptamer-conjugated AuNPs which selectively bound to the surface of target cells, acted as micro-meter size gold structure. Therefore, the scattering and absorption read-out was significantly changed compared to complex control samples (Medley et al., 2008), but this could be useful for imaging rather than detection due to its low sensitivity.

The second format is based on the networking of AuNPs by sandwich binding (Fig. 1a,b). The formation of AuNPs network results in a red-to-purple color change due to the decreasing of AuNP inter-particle distance. Some proteins comprise two or more equivalent epitopes like platelet-derived growth factor (PDGF) that is a homo-dimeric protein which can be used to create AuNPs cross-linked by aptamers bridges with PDGF protein (Huang et al., 2005). With this format, platelet-derived growth factor receptor (PDGFR) could be detected as low as 3.2 nM of LOD by the competitive binding of PDGF aptamer and PDFGR to PDGF. However, as mentioned above, this sandwich-type binding assay has still been limited in its full expansion to all of target molecules, mainly due to the lack of available dual aptamers. Unfortunately, just very few of dual aptamers available for the targets have been reported to date, because, we believe, in normal SELEX processes it is very difficult to isolate the two aptamers binding to the different sites of a target, due to the limited exposure of the target's surfaces since the targets are immobilized on solid support. Although Gu's group have developed a new SELEX process using graphene-oxide (Park et al., 2012) which can obtain dual aptamers with target-free immobilization method, and demonstrated a sandwich detection for several targets, the dual aptamers development for small molecular targets such as small organic or inorganic compounds are not applicable in this GO-SELEX method (Ahmad Raston and Gu, 2015; Kim and Gu 2014; Kwon et al., 2015; Nguyen et al., 2014; Park et al., 2014). To overcome this limitation, the target induced displacement scheme using complementary DNA has been proposed to construct AuNP network-based colorimetric aptasensors. Lu's group have reported several colorimetric aptasensors based on this strategy. Here, two DNA probes partially complemented to parts of aptamer that were individually immobilized on AuNPs. Thus, the aptamers led the networking of AuNPs by hybridization between two probe DNAs and aptamers in the absence of target, resulting in red-to-purple color change. In the presence of target, the network of AuNPs was destroyed by the binding of aptamers to targets, resulted in of the purple-to-red color change. By using this method, adenosine and cocaine were simply detected via naked eye (Liu and Lu, 2006). In this approach, the complementary sequences should be sophisticatedly designed, depending on the sequence of the aptamer and its affinity, because the analytical performance is quite dependent on the competitive interaction among aptamer, complementary DNAs, and the target. Another example of colorimetric sensing based on AuNP networking is the detection method of metal ions such as Hg^{2+} and Ag^{+}. Thymine–thymine (T–T) and cytosine–cytosine (C–C) mis-matching can be stabilized in the presence of Hg^{2+} and Ag^{+} by formation of T–Hg^{2+}–T and C–Ag^{+}–C, respectively (Ono et al., 2011). This phenomenon was successively applied in colorimetric metal ion detection (Lee et al., 2007; Xu et al., 2012). In this method, T-rich or C-rich oligonucleotides were functionalized on AuNPs that were aggregated by formation of T–Hg^{2+}–T and C–Ag^{+}–C, in the

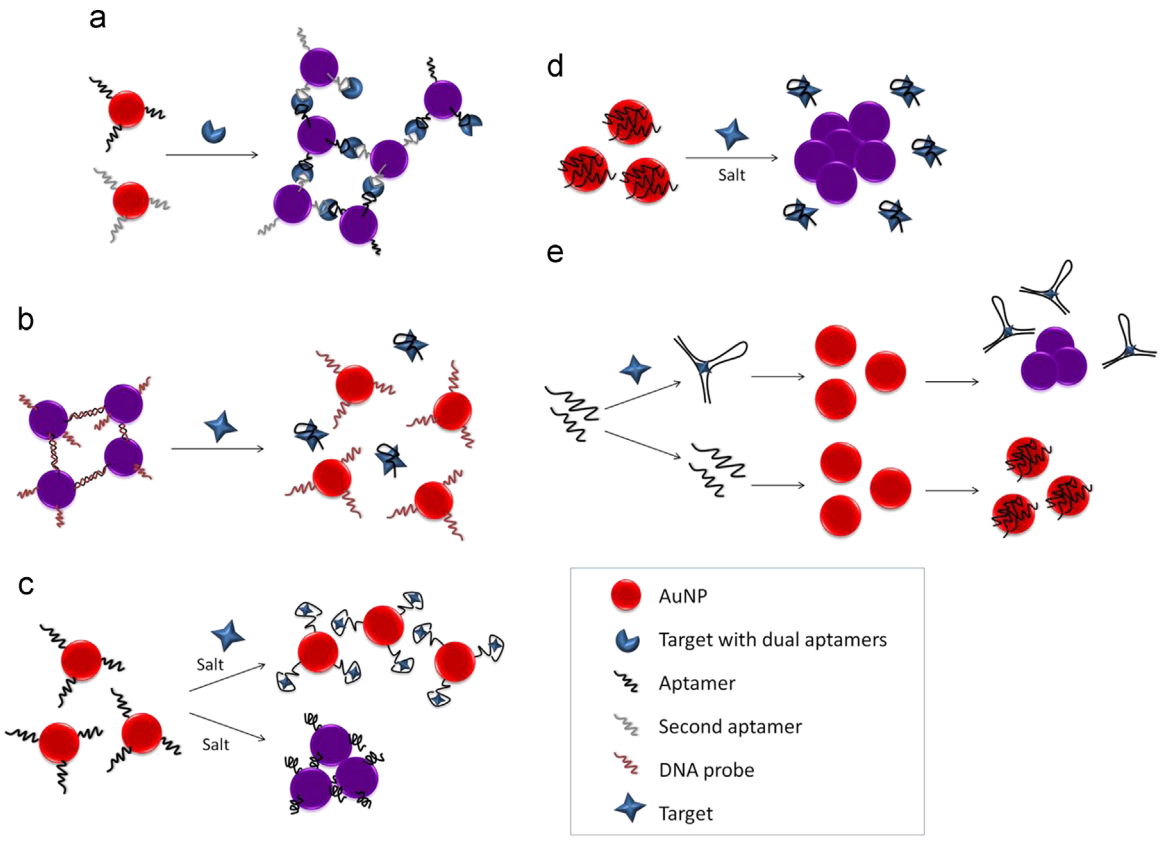

Fig. 1. Colorimetric aptasensors using modified (a–c) and unmodified (d and e) AuNPs. (a) Sandwich-type colorimetric aptasensors using dual aptamers; (b) target-induced displacement of aptamer from AuNPs network; and aggregation of AuNPs via surface condition using (c) DNA folding effect; (d) target-induced conformational change of aptamer and (e) target-induced assembly of aptamer fragments.

presence of Hg^{2+} and Ag^{+}. Thus the color of AuNPs solution was changed from red to purple. This method is very powerful in the detection of Hg^{2+} and Ag^{+}, but the analytical performance could be quite affected by the sample quality. Many organic or ionic components in real samples can interfere the interaction between metal ions to aptamers.

The last strategy is based-on the aggregation of AuNPs via the control of surface conditions (Fig. 1c–e). AuNPs in suspension is generally stabled by adsorption of anions on their surfaces. This induces the electrostatic repulsion between AuNPs that is stronger than van der Waals attraction force between AuNPs. Salt normally induces the aggregation of AuNPs because it reduces the electrostatic repulsion between AuNPs. But, the functionalization of AuNPs with ssDNA protects the aggregation of AuNPs at even higher concentration of salt condition. Li and co-workers proposed a colorimetric aptasensor based on non-cross-linking AuNP aggregation (Zhao et al., 2007) which then was adopted in the detection of adenosine and adenosine deaminase using adenosine binding aptamer immobilized AuNPs (Zhao et al., 2008).

Besides the use of ligands modified-AuNPs, Li and Rothberg proposed a new strategy of colorimetric sensing using unmodified AuNPs for DNA detection, which is depending on the differential electrostatic interaction of ssDNA and dsDNA to AuNPs. The adsorption of ssDNA on AuNPs protects the aggregation of AuNPs at salt condition. Inspired by this discovery, a number of colorimetric aptasensors using unmodified AuNPs have been developed based on target induced conformational change of aptamers (Chang et al., 2013; Gopinath et al., 2014; Kim et al., 2010b; Liu et al., 2008; Wang et al., 2006; Wei et al., 2008).However, this approach cannot be applied for all available aptamers because some aptamers are unable to undergo a sufficient conformational change upon target binding. Hence, Fan and co-workers proposed a colorimetric aptasensor using unmodified AuNP based on target induced displacement format, where AuNPs were stabilized by the adsorption of complementary ssDNA, detached from the aptamer duplex structure upon the binding of aptamer to target (Wang et al., 2007).With similar approach, stabilizing DNA probe was also used to protect the binding of aptamer to AuNPs by stabilizing aptamer conformation. More advanced strategy based on the splitting of aptamer sequence to two segments was reported by Fan and co-workers (Zhang et al., 2008b). More recently, Gu's group suggested the signal enhancement method for unmodified AuNPs based colorimetric aptasensors by the modulation of interaction between aptamers and AuNPs through the exchange of capping agents of AuNPs when aptamers having low affinity to targets are used (Kim et al., 2011). Instead of complementary DNA, cationic polymer (diallyldimethylammonium chloride, PDDA) was also used in umAuNP-based colorimetric aptasensor with same approach of above report (Jeon et al., 2013). This unmodified AuNPs-based colorimetric aptasensors is very useful for on-site detection due to its excellent simplicity, but its accuracy and repeatability is slightly lower than the aptamer modified AuNPs assay, because the interaction between aptamers and AuNPs is rather delicate depending on the sensing environments. Therefore, this method is more suitable to qualitative assay, not quantitative analysis.

2.3. *Fluorometric sensing*

Fluorometric sensing is more promising methodology to analyze the biomolecular interaction and measure them quantitatively and sensitively compared to colorimetric assay (Chen et al., 2008; Jung et al., 2007). A number of fluorescence and quenching materials are available and easily conjugated with aptamers. High flexibility in aptamer conformation is very useful for conducting

various types of fluorescence aptasensors, such as aptabeacon using hairpin structured aptamer (Frauendorf and Jaschke, 2001; Yamamoto et al., 2000) aptamer-based fluorescence resonance energy transfer (FRET) assay (Liu et al., 2009a; Ozaki et al., 2006; Song et al., 2009; Stojanovic et al., 2001), target-induced displacement fluorescence assay (Cruz-Aguado and Penner, 2008; Nutiu and Li, 2003), intercalating dye-based label-free fluorescence assay (Xiang et al., 2009; Xiang et al., 2010; Xu et al., 2009b), and eximer signaling method (Wu et al., 2010).

More recently, AuNPs have been widely used in the fluorometric aptasensors based on the superquenching property of AuNP for almost of fluorescence materials (Liu et al., 2014). The quenching effect of AuNP represents orders of magnitude higher than one of other organic quenching molecules (Fan et al., 2003; Liu et al., 2007a). Based on these quenching properties of AuNP, Chang and co-workers developed FRET based aptasensor using AuNP for the detection of PDGF (Huang et al., 2007). This method showed high sensitivity for PDGF detection as low as 8 pM LOD. Chang's group also proposed another scheme of fluorescence aptasensor for same target using two different sized AuNPs, small sized AuNPs (2 nm in diameter) were conjugated with PDGF as a donor and large sized AuNPs (13 nm in diameter) were functionalized with PDGF aptamers as an acceptor (Huang et al., 2008). In the absence of PDGF, both AuNPs were linked via the interaction of aptamer to PDGF thus the photoluminescence of 2 nm AuNPs were quenched by the 13 nm AuNPs. The photoluminescence signal was recovered by the addition of free PDGF that caused the breaking of sandwich linkage by competitive binding, resulted in the sensitive PDGF detection as low as 80 pM LOD. This assay was further applied to clinical samples of urine from healthy people and demonstrated excellent analytical performance. This approach is very sensitive, but a high performance optical instrument is essential for the detection of FRET signal from small AuNPs.

Zhao and co-workers investigated three strategies of FRET-based aptasensors depending on the different methods for the releasing of fluorescence dye from AuNPs (Wang et al., 2008) as can be seen in Fig. 2. In the first approach, thrombin induced the displacement of fluorescent dye labeled complementary DNA by the binding to aptamers immobilized on AuNPs thus the fluorescence signal was restored. Second approach adopted thrombin binding caused the detachment of aptamers from non-labeled complementary conjugated on AuNPs thus the fluorescence signal was recovered. This aptasensor was a very straightforward and fast, but the non-specific adsorption should be solved to achieve a high sensitivity and reproducibility compared to above two strategies. The first method showed higher sensitivity (0.14 nM LOD) than one of second method (3.78 nM LOD), which could be caused by the differential non-specific adsorption of aptamer-thrombin complex and complementary DNA to the surface of AuNPs. But, this result in sensitivity might be quite depending on the electrostatic properties of target/aptamer complex and design of complementary DNA.

AuNP has a broad quenching ability for various fluorescence dyes, which is useful for multiplex detection without sophisticated design and optimization of acceptor–donor pairs (Song et al., 2009). Fan and co-workers proposed a multicolor fluorescent AuNP based on target induced displacement format in aptasensors (Zhang et al., 2010). In this report, three different aptamers for small molecular targets (adenosine, cocaine and potassium ion) were labeled with three kinds of fluorescence dyes (Rox, Cy5 and FAM), respectively, and AuNPs were functionalized with three DNA probes that were complemented with a part of three aptamers, respectively. In the absence of targets, just small background fluorescence at all three wavelengths corresponding to dyes was emitted by simultaneous quenching of all dyes to AuNPs. Upon the addition of each target, aptamers were released from AuNPs, resulting in increasing of fluorescence signal at corresponding wavelength. Recently, Kim and Jurng simplified this approach with the combination of AuNPs as a quencher and quantum dots (QDs) as a donor to generate three different fluorescence signals by single-laser excitation (Kim and Jurng, 2011). This report described in detail at following section about QDs-based aptasensors.

2.4. Electrochemical sensing

To date a number of papers have described electrochemical aptasensors based on various strategies, such as simple binding of aptamers to targets (Kim et al., 2009b; Radi et al., 2005; Rodriguez et al., 2005; Xu et al., 2006), target induced conformational change (Baker et al., 2006; Xiao et al., 2005; Zuo et al., 2007), target induced displacement format using complementary DNA (Du et al., 2008; Lu et al., 2008; Wu et al., 2007; Xiao et al., 2007), and applications of intercalating redox molecules like methylene blue (Feng et al., 2008; Ferapontova et al., 2008). But, the sensitivity of these electrochemical aptasensors was not sufficient to apply them in real samples, especially small molecular targets like antibiotics (Kim et al., 2010a).

The incorporation of AuNPs in electrochemical aptasensors has

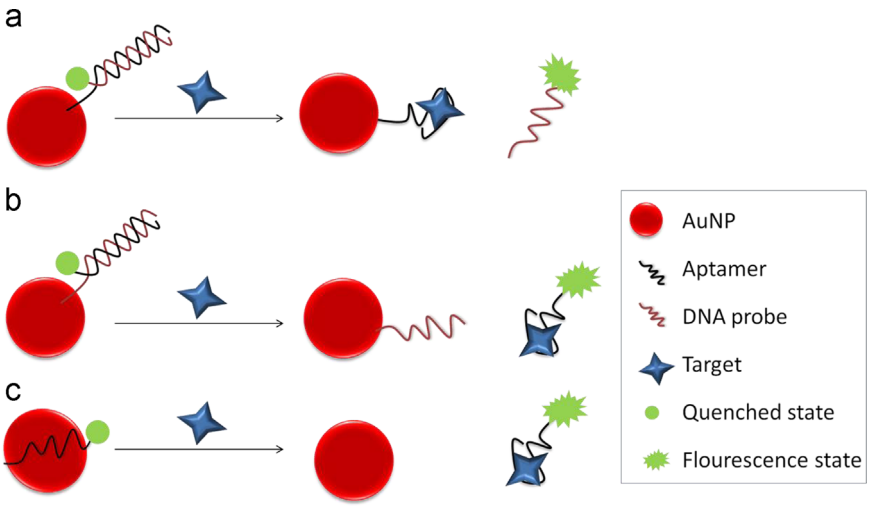

Fig. 2. Fluorescent aptasensors using AuNPs as fluorescence quencher. Fluorescent assay using modified AuNPs based on (a) target-induced displacement fluorescent dye-labeled complementary DNA; (b) target-induced displacement of aptamer from non-labeled complementary DNA; and (c) target-induced conformational change of aptamer and detached from unmodified AuNPs.

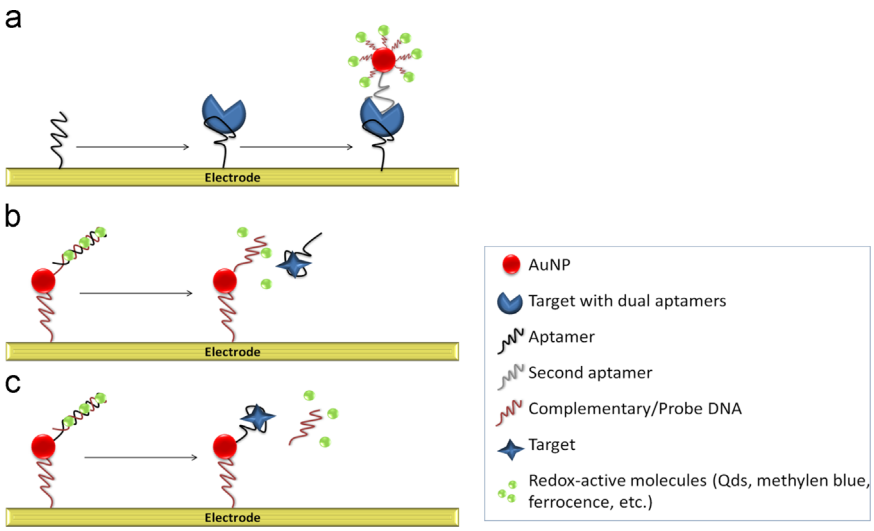

Fig. 3. Electrochemical aptasensors using AuNPs for signal amplification. Electrochemical assay based on sandwich format using (a) dual aptamers and aptamer-probe DNA hybrid (b and c).

the potential to amplify electrochemical signal based on properties of AuNPs such as large surface area and high redox activity. The strategies of electrochemical signal enhancement using AuNPs can be classified into two approaches (Du et al., 2010). The first approach is the enlargement of electrode surface by attachment of AuNPs on electrode, which might increase the amount of capture probes on electrode thus the electrochemical signal intensity can be enhanced. The second approach is the use of AuNPs as a label for the amplification of electrochemical signal (Fig. 3). Zhang and co-workers developed a sensitive electrochemical aptasensor for cocaine detection using by self-assembled AuNPs on a gold electrode (Li et al., 2008b), followed by similar approach demonstrated using the complex of AuNPs and $Ru(bpy)_3^{2+}$ (electrochemiluminescence substrate) (Wang et al., 2010a).

Dual aptamers for thrombin were also applied in this sandwich based electrochemical aptasensors and showed a good analytical performance (20 pM LOD) (Li et al., 2008a). Latest report came into literature on electrochemical aptasensor addressing the successful development of gold-nanostructured graphite screen-printed electrode using alkaline phosphatase for the rapid detection of vascular endothelial growth factor (VEGF). In this study, dual aptamers has greatly assisted the successful device fabrication, where the printed electrode was modified with thiolated primary aptamer as target capturing probe and secondary biotinylated aptamer was conjugated with streptavidin-alkaline phosphatase to catalyze the hydrolysis of electroinactive 1-naphthyl-phospahte to electroactive 1-naphthol, detected for signal response. The LOD for VEGF detection was found to be 30 nmol/L. In addition, this aptasensor performance provided POC diagnosis of VEGF as cancer biomarker (Ravalli et al., 2015). As mentioned above, however, dual aptamer based sandwich detection is limited to certain targets only, due to the lack of available dual aptamer pairs. Therefore, many of electrochemical aptasensors with the sandwich format comprised aptamers and complementary DNA where the electrochemical signal was changed by the displacement of aptamer/AuNP in the presence of target (Ding et al., 2010a; Du et al., 2009; Shen et al., 2007; Zhang et al., 2008c). Next, Willner's group reported another electrochemical aptasensor using splitted aptamers for cocaine detection (Sharon et al., 2009). Wang and co-workers proposed an ultrasensitive electrochemical aptasensor using dual labeled AuNPs with enzyme and aptamer for the detection of MUC1, epithelial tumor marker (Hu et al., 2014). In this study, AuNPs were conjugated with hairpin structured MUC1 binding aptamer labeled with biotin and horseradish peroxidase (HRP). In the presence of target, hairpin structure of aptamer was stretched by binding to MUC1 thus AuNPs/aptamer/HRP complex was immobilized on streptavidin modified electrode by the binding of biotin at the end of aptamers. As a result, an electrochemical signal was increased by the generation of electrolytic molecules by HRP. In the absence of target, AuNPs/aptamer/HRP was not captured on electrode because a biotin at the end of aptamer was not hidden by AuNP due to the hairpin structure of aptamer. The sandwich-type electrochemical aptasensor is very suitable in field because the direct generation and amplification of the electrochemical signal by enzyme or labeled DNA/metallic particles is most preferable in real application like glucose sensor. The signal-off method such as the current decreasing upon the target binding, however, is not feasible in real field, not only it requires many negative control samples, but also it needs mediator treatment.

2.4.1. *Magnetic nanoparticles*

Magnetic nanoparticles enable to amplify the signal by simple concentration of targets using magnet. More importantly, the specificity of biosensors can be improved by the elimination of various interfering elements in biological samples (Bamrungsap et al., 2012). Therefore, magnetic nanoparticles, especially magnetite (Fe_3O_4) nanoparticles having superparamagnetic property, are commonly used in bio-analysis system for the separation and signal producing. Recently, many reports about aptasensors using magnetic nanoparticles alone or coupled with other nanomaterials have been introduced.

Song and co-workers developed rapid and ultra-sensitive aptasensors for the detection of adenosine monophosphate (AMP) based on dual aptamer conjugated particles system (Song et al., 2009). They designed two DNA probes that were partially complemented with AMP binding aptamer, and two DNA probes were functionalized on magnetic particles and fluorescence nanoparticles (FNPs), respectively. In the absence of AMP, FNPs were coupled with magnetic particles via sandwich binding between two DNA probes on particles and AMP binding aptamers. While, the FNPs assembled on magnetic particles departed from magnetic particles due to the breaking of hybridization by AMP-aptamer interaction in the presence of AMP. As a result, 0.1 μM of LOD for AMP quantification was achieved based on the merits of the separation and signal amplification by aptamer/magnetic particle conjugates. This sensitivity was highly improved, compared to the previous colorimetric assay for AMP detection, although several steps are required additionally. Tan and co-workers demonstrated

the detection of acute leukemia cells (Herr et al., 2006; Zhao et al., 2003). Specific aptamers against acute leukemia cells were conjugated to MNPs and $[Ru(bipy)_3]^{2+}$ doped nanoparticles for separation and signal generation, respectively. The combination of two aptamer conjugated nanoparticles enabled to perform selective cell separation from complex biological samples and detect them with high sensitivity for short incubation time. This dual aptamer functionalized nanoparticles system was expanded to multiple cell isolation and detection (Smith et al., 2007). Three aptamers for three different types of cancer cells (CCRF-CEM acute leukemia cell, Ramos cell, and Toledo cell) were respectively functionalized to MNPs and dye-doped nanoparticles. Cells in samples were isolated using aptamer/MNPs conjugates, then they detected them by the addition of aptamer/ dye-doped nanoparticle conjugates. The application of MNPs for cell detection and imaging is very useful because the simple isolation and concentration of the specific cells by MNPs can enhance both the sensitivity and selectivity for cell analysis. MNPs were used in coupled with AuNPs to develop the sensitive thrombin detection based on sandwich assay format (Zheng et al., 2007). The MNPs and AuNPs were modified with thrombin binding aptamers, respectively. A sandwich binding between two particles and target was formed in the presence of thrombin. Additionally, thiocyanuric acid was added for signal amplification as low as 7.82 aM of LOD.

It was already known that MNPs have an intrinsic peroxidase-like activity in the presence of hydrogen peroxide (Gao et al., 2007), and some colorimetric assay based on this function of MNPs were reported for the detection of various targets such as glucose, proteins, carbohydrates and DNA (Ding et al., 2010b; Gao et al., 2008; Park et al., 2011; Yu et al., 2009). Recently, a colorimetric aptasensor based on this catalytic activity of MNPs was demonstrated (Kim and Jurng, 2013). As shown Fig. 4, the positively charged surface of MNPs was screened with aptamers by an electrostatic adsorption, thus the catalytic activity of MNPs was reduced because the adsorbed aptamers on the surface of MNPs prevent the access of substrates to the surface of MNPs. By the addition of target, the peroxidase like activity of MNPs was restored by the displacement of aptamers from MNPs, resulted in the color change of substrate solution due to their degradation. Although this report demonstrated a novel application of MNPs as signal generator, not separation/concentration tool for aptasensor development, high background signal appeared in absence of target should be solved in order to be widely used.

2.4.2. Gold nanorods

One of widely used non-spherical nanomaterials for biosensor application is the gold nanorod (Ma and Ding, 2009; Sreeprasad et al., 2008). Compared to AuNPs, gold nanorods have two featured properties, large surface area and dimensional anisotropy (Castellana et al., 2010). A large surface area of gold nanorods is profitable to develop sensitive biosensors for complex targets because many receptors can be immobilized on the surface of gold nanorods. Tan and co-workers demonstrated that about 80 fluorophore-labeled aptamers were immobilized on the surface of single nanorod (12 nm × 56 nm size) (Huang et al., 2008). This enabled to enhance a fluorescence signal and reinforced the interaction with target cells via multivalent binding compared to single dye-labeled aptamers.

Gold nanorods are also suitable materials for surface enhanced Raman scattering (SERS). A particle shape plays important role in enhancing Raman scattering signal. It was already reported that the adsorbed molecules on gold nanorods showed a high enhancement factor of 10^4–10^5, while a similar result was not observed for AuNPs (Nikoobakht et al., 2002). Therefore, high sensitive SERS-based biosensors using gold nanorods can be accomplished. For instance, recently Irudayaraj and co-workers introduced a novel SERS-based aptasensor using both of gold nanorods and AuNPs (Wang et al., 2010c). In this study, gold nanorods were conjugated with thrombin antibodies and AuNPs were functionalized with thrombin aptamers-labeled Raman reporter that binds to another region of thrombin with antibodies. In the presence of thrombin, gold nanorods and AuNPs were closed by sandwich binding among thrombin, aptamers and antibodies, generating SERS hot spots. The detectable SERS signal was not observed in the absence of thrombin in this method. This SERS-based aptasensor showed high sensitivity for the detection of thrombin as low as 887 pM in 5% human serum samples. This approach can be expanded for multiplex detection using multiple aptamer/SERS reporter combinations. Even though the gold nanorod-based SERS assays have shown good analytical performance, it requires not only a sophisticated instrument for analysis but the analytical performance is also quite delicate to analysis conditions. So, it could be more suitable to bioanalysis study, not a simple biosensor platform.

2.5. Carbon and silica nanomaterials-based aptasensors

2.5.1. Single walled carbon nanotubes

Aside from nanoparticles, other shapes of nanomaterials have been applied for the bioanalysis. Among them, single walled

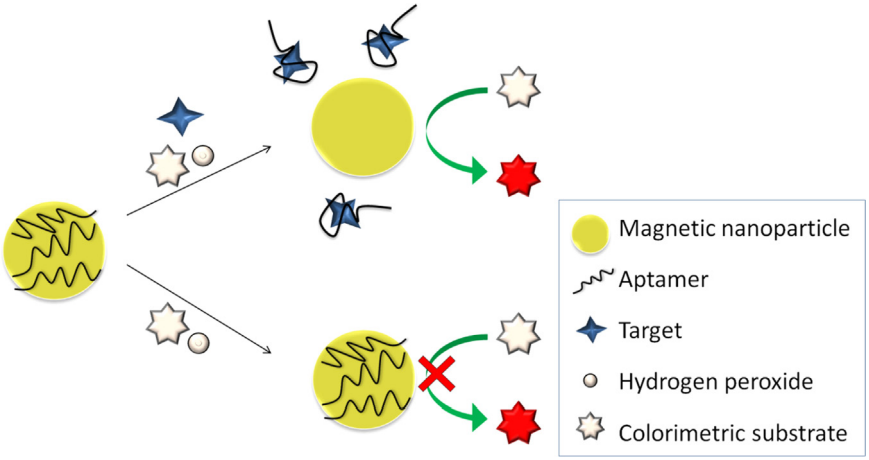

Fig. 4. Colorimetric aptasensor based on catalytic activity of MNPs. A simple colorimetric assay for metal ions detections based on peroxidase-like activity of MNPs and aptamer.

carbon nanotubes (SWCNTs) have been extensively studied for the biosensor application based on the excellent material properties such as high surface area, mechanical strength, thermal and electrical conductivity (Ajayan, 1999). These properties of SWCNTs offer the possibility that SWCNTs can be used as transducer elements in biosensor system. The semiconducting SWCNTs can be converted from a conducting to insulating state in field-effect transistor (FET). Lee and co-workers firstly reported the SWCNT-FET biosensor using aptamers (So et al., 2005). In this study, anti-thrombin aptamers were covalently immobilized on the side-walls of SWCNTs which were modified with carbodiimidazole-activated Tween 20 (CDI-Tween 20). This SWCNT-FET aptasensors detected the thrombin as low as 10 nM by measuring conductance. The authors claimed that the size of receptors is critical to the performance of sensors because the interaction between receptors and targets should be occurred within electrical double layer in milli-molar salt concentration to generate the conductance change. In aspect of this point, antibodies are not suitable in FET biosensors, while aptamers are good receptors in FET biosensors due to their small size (a few nanometer) and excellent recognition ability. It was further demonstrated that aptamers are more proper in SWCNT-FET biosensors than antibodies by Tamiya's group (Maehashi et al., 2007). In this study, aptamer-functionalized SWCNT-FET showed better results for immunoglobulin E (IgE) detection than those produced by IgE antibodies conjugated SWCNT-FET under similar conditions. The SWCNT-FET aptasensors were also applied for the bacteria detection with high sensitivity and selectivity. Lee and co-workers developed the aptamer immobilized SWCNT-FET array chip for the *Escherichia coli* detection in water (So et al., 2008). In this system, the conductance was decreased as much as 50% by the binding of *E. coli* to RNA aptamers immobilized on SWCNT. More impressively, the conductance change of aptamer-functionalized SWCNT-FET was not noticeable in the presence of high density *Salmonella typhimurium*. The SWCNT-FET based aptasensors showed excellent sensitivities for various targets, but there are some unsolved critical problems in real application. The most critical defect is its low reproducibility in assay. The preparation of well-qualified SWCNT-FET chips with high uniformity is still not easy at every different lot produced. Zelada-Guillen et al. developed the SWCNT-based potentiometric aptasensor using an RNA aptamer specific to IVB pili of *Salmonella typhi* which is a major cause of food poisoning in many cases worldwide (Zelada-Guillen et al., 2009). This aptasensor detected *S. typhi* as low as 0.2 CFU/ml with wide dynamic range. Also, they were simply regenerated by the treating 2 M NaCl for 30 min, which lead the breaking of interaction between aptamers and IVB pili of *S. typhi*. Since this report, the same group expanded this system to other microorganisms. In 2010, the SWCNT-based potentiometric aptasensor was developed for the selective detection of *E. coli* in complex matrix such as milk and apple juice (Zelada-Guillen et al., 2010). This aptasensors also well discriminated the *E. coli* from other microorganisms such as *Salmonella enterica*, *Lactobacillus casei*, and other sub-type of *E. coli*. In 2012, SWCNT-based potentiometric aptasensor was developed for the detection of *Staphylococcus aureus* (Zelada-Guillen et al., 2012). In this aptasensors, a tailored DNA aptamer against two epitopes on the surface of *S. aureus* was used (Cao et al., 2009), and new approach for aptamer conjugation on SWCNT was developed. Aptamers were modified with pyrenil moieties at the 3' end, then they were directly adsorbed on the side-walls of SWCNT side walls via strong p-stacking interaction between the pyrenil groups of aptamers and the side-walls of SWCNT. As mentioned in SWCNT-FET aptasensors, however, the preparation of well-controlled SWCNT-potentiometric chip is still very important for high reproducibility.

It was discovered that SWCNTs have a quenching effect when they are coupled with variety of fluorescent elements such as fluorophores and quantum dots (Cui et al., 2008). Besides, SWCNTs interact to single-stranded DNA (ssDNA) and double-stranded DNA (dsDNA) with different patterns (Gigliotti et al., 2006; Zhao and Johnson, 2007). The ssDNA wrap around SWCNTs through π–π stacking interactions between the bases of ssDNA and the side-walls of SWCNTs, whereas dsDNA is interacted with SWCNTs depending on the surface charge of SWCNTs because the bases of dsDNA are hidden inside of double-helix structure, which is distinguished by π–π stacking interaction. This phenomenon can be applied in SWCNTs-based aptasensors because the structure of aptamers is flexible as stretched ssDNA or well-defined 3-D conformation containing stem regions depending the absence or presence of targets. Based on above two properties of SWCNTs, a fluorescent aptasensor using SWCNTs and dye-labeled aptamers was developed (Zhu et al., 2008). In this report, thrombin aptamer was labeled with Chlorin e6 (Ce6), a photosensitizer. In the absence of thrombin, aptamers wrapped around the surface of SWCNTs, which resulted in the quenching of a singlet oxygen generation of Ce6 due to the close proximity of Ce6 to the surface of SWCNTs. While thrombin aptamers were detached from SWCNTs in the presence of thrombin due to the conformational change of aptamers, resulting in a recovery of a singlet oxygen generation of Ce6. Kang and co-workers reported a near-infrared (NIR) optical aptasensors based on the NIR adsorption and photoluminescence properties of SWCNTs (Chen et al., 2009a). In the absence of thrombin, SWCNTs were dispersed due to the wrapping of aptamers onto the surface of SWCNTs, which led sharp peaks in the absorption spectrum. Otherwise, the aptamers were detached from SWCNTs by the addition of thrombin, resulting in an aggregation of SWCNTs. Aggregated SWCNT solution showed different NIR absorption spectrum with homogenous dispersed SWCNT solution. In this label-free and single-step assay, thrombin was detected as low as 0.1 nM. Although many sensitive SWCNT-based FRET aptaensors were developed to date, researchers are more interested in graphene recently as quenching materials, instead of SWCNT, due to the high surface area of graphene.

2.5.2. Graphenes

Graphene materials including graphene oxide (GO) are one of most fascinating nanomaterials in recent years for the applications in biosensors due to their unique electronic, optical and mechanical properties (Yao et al., 2012). In addition, ssDNA is well adsorbed on the surface of graphene and GO by π–π stacking interaction compared to dsDNA. Therefore, the combination of graphene materials and aptamers has supplied a high potential to develop the novel graphene-based aptasensors (Ping et al., 2015). Graphene has an excellent fluorescence quenching capability for numerous fluorophores due to intrasheet energy or electron transfer. Especially, GO is more commonly used in FRET-based aptasensors because it is well dispersed in water due to its hydrophilic nature (Chen et al., 2012b). Recently, many researchers reported FRET-based aptasensors using GO as a quencher for the detection of various targets (Wang et al., 2010b; Zhao et al., 2013). As depicted in Fig. 5, fluorescence dye labeled aptamers were adsorbed on GO nanosheets, and the fluorescence signal was quenched. By the addition of targets, then the aptamers were displaced from GO surface by target induced conformational change of aptamers to folded structure, resulting the increasing of fluorescence signal. This assay was applied to not only *in vitro* analysis, but also *in vivo* molecular probing of ATP (Yi et al., 2014). Instead of fluorescence dyes, QD was also used for GO-based FRET aptasensors (Zhou et al., 2014). In this paper, QD was conjugated with aptamers and QD/aptamer conjugates were adsorbed onto GO. The released QD by the binding of targets (carcino-embryonic antigen) were analyzed by laser-induced fluorescence-coupled affinity probe capillary electrophoresis. As abovementioned,

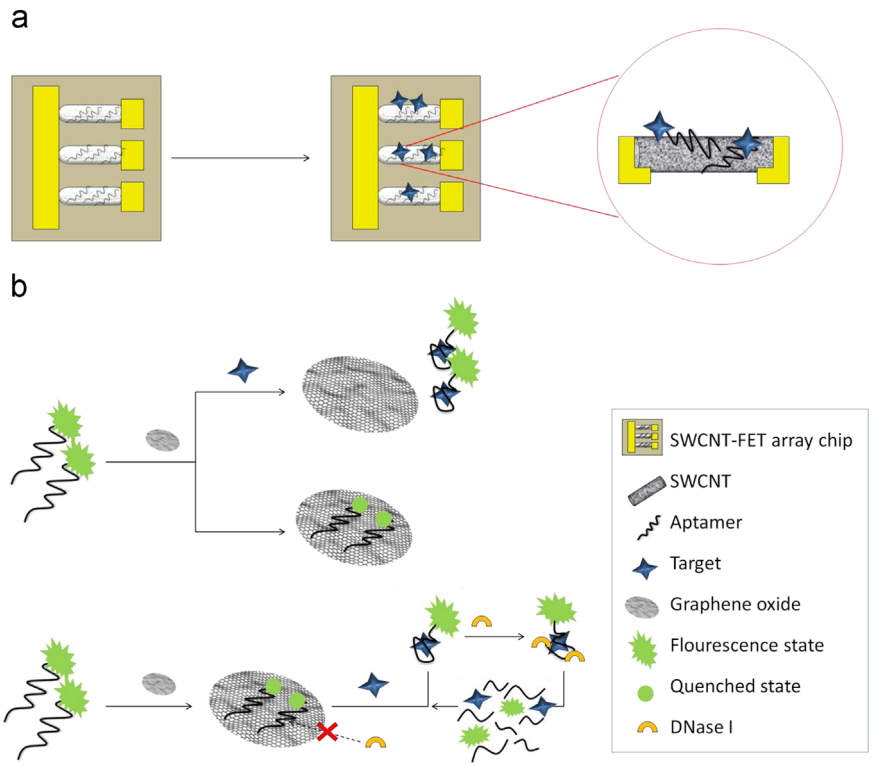

Fig. 5. Carbon nanomaterials-based aptasensors. (a) Aptamer-functionalized SWCNT-FET aptasensor and (b) FRET-based aptasensors using GO as quencher using catalytic recycling of analyte for signal amplification.

however, this method could not suppose to be applicable to all aptamers because conformational change of aptamers is quite depending on aptamer sequence. To generalize this approach, the interaction between aptamers and graphene oxide nanosheets was controlled in FRET-based aptasensors using complementary DNA based on the target induced displacement manners (Pu et al., 2012). However, more comprehensive understanding on the competitive interaction among aptamer, graphene and target is required to improve this method. For this purpose, Liu and co-workers have studied the effect of solution pH on the interaction between aptamers and GO as well as the binding of aptamers to targets (Huang et al., 2011). They claimed that these two interactions can be modulated by adjustment of solution pH to enhance the sensitivity, which is a similar to the concept of Gu's group report about umAuNPs based colorimetric aptasensors (Kim et al., 2011). A covalent immobilization of aptamer on GO is available approach to overcome the susceptible interaction between aptamer and GO. In addition, non-specific displacement of physisorbed aptamers on GO raised a false positive signal. Liu and coworker compared the fluorescence signal between covalently immobilized aptamers on carboxylate GO and physisorbed aptamers on GO (Liu et al., 2014c). As a result, the sensitivity of both aptasensors was similar, but the background signal of the assay using covalently bound aptamers was lower than that of physisorbed aptamer-based assay. This covalently bound aptamer-based assay showed much better sensitivity, especially intracellular analysis, because covalently linked aptamer on GO was protected from nuclease.

The effective adsorption of aptamers on GO was expanded to surface plasmon resonance (SPR)-based aptasensors (Subramanian et al., 2013; Wang et al., 2011b). In this assay, GO was assembled on SPR Au film via electrostatic interaction. Then, aptamers were adsorbed onto GO surface. Although the sensitivity of this assay was not remarkable compared to other platforms, this approach is meaningful, demonstrating that SPR system could be used for small molecular detection, since SPR platform is known to be not effective for small molecules inherently.

Furthermore, GO have been used as blocking materials against the enzymatic degradation of biomolecules, or rolling circle amplification. Several signal amplification strategies were incorporated to the feature of GO's steric hindrance to enhance the sensitivity. One effective strategy is to use the nucleases into the sensing process. For example, Chen's group proposed a novel signal amplification method in GO-based aptasensor using enzymes (DNase I or Exonuclease III) (Chen et al., 2012a; Lu et al., 2010). In this sensing process, dye-labeled aptamers adsorbed on GO could be protected from the degradation by enzyme. By the addition of target, aptamers were detached from GO, then they were degraded by enzyme and targets were released from aptamers. These free targets were cycled to detached more aptamers from GO. Therefore, the signal could be amplified by repeated enzyme reaction. As a result, 250-fold enhancement of sensitivity was achieved by this method. As a similar strategy, rolling circle amplification was applied in GO-based aptasensors (Liu et al., 2014b). In this method, target induced displacement of aptamers from GO was amplified and detected. The sensitivity of this assay was competitive, compared to well-defined bioluminescence assay for ATP detection, but the primer binding sequence tagged to aptamer should be well designed, which might be considered as a key to the performance. The signal amplification approach by coupling GO and enzyme is very interesting due to its concept and sensitivity. If the interaction of GO and aptamer is also well controlled in field, not laboratory, it could be commercialized quickly. The excellent quenching capacity of GO enables long range resonance energy transfer (LrRET) for fluorescence sensing (Zhuang et al., 2013). Hibino and co-workers proposed a LrRET based aptasensor using DNA spacer modified aptamers and GO (Ueno et al., 2013). They optimized the length of DNA spacer of aptamer for LrRET and achieved 1 nM of LOD for thrombin detection. More interesting application of GO in aptasensors is a multiplexed detection (Wang et al., 2014; Wu et al., 2012). In these studies, two

fluorescence dyes were conjugated to their two different aptamers and aptamers, respectively, and they were simultaneously quenched by the adsorption of aptamers on single GO nanosheet. To construct GO-based multiplex aptasensors, a paper-based microfluidic biochip integrated GO and aptamer and tunable GO-microarray have been also developed for multiple proteins or microorganisms detection (Jung et al., 2013; Zuo et al., 2013). GO has been applied in chemiluminescent (CL) aptasensors based on its excellent CL quenching ability through chemiluminescent resonance energy transfer (CRET) with similar approaches of FRET-based aptasensors (Choi and Lee, 2013; Song et al., 2014). GO has been also used as an electron donor in FRET-based aptasensors (Shi et al., 2013). In this aptasensor, cocaine aptamer was conjugated with both of GO (donor) and AuNP (acceptor). In the presence of cocaine, GO was closed to AuNP by the folding of cocaine aptamer into a three-way junction, resulting in the decrease of fluorescence signal of GO. With similar approach, T-rich DNA conjugated GO was used to detect mercury ions (Li et al., 2013). In this method, Hg^{2+} was bound to T-rich DNA by the formation of T–Hg^{2+}–T, which led close proximity of Hg^{2+} to GO, consequently the fluorescence of GO was quenched by Hg^{2+} through electron transfer from GO along the duplex DNA channel.

Researchers have an intensive interest in the application of graphene as transducer or carrier of redox molecules in electrochemical aptasensors. Graphene has excellent properties as electrochemical transducer such as wide electrochemical window and fast electron transfer kinetics (Huang et al., 2012). Based on these properties, Li and co-workers developed graphene-based electrochemical aptasensor for the detection thrombin (Zhao et al., 2011). In this study, aptamers were physically adsorbed on the surface of graphene/QD composites and $[Fe(CN)_6]^{3-/4-}$ was used as redox molecules on the graphene/QD composite modified pyrolytic graphite electrode. In the absence of thrombin, aptamers adsorbed on graphene surface interfered the electron transfer between electrode and $[Fe(CN)_6]^{3-/4-}$. The current was increased by displacement of aptamers from graphene modified electrode in the presence of thrombin. Similarly, a graphene-based FET like aptasensor was developed (Xu et al., 2014). Methylene blue (MB) or QD-labeled thrombin aptamers were immobilized onto graphene covered Si/SiO2 wafer. Interestingly, in this study, thrombin aptamer was used to detect lead and potassium ion. In the presence of target ions, the conformation of thrombin aptamer was changed from stretched form to folded structure, consequently MB or QD was closed to graphene, resulting in a change of the electrical signal. A high-throughput and reusable electrochemical aptasensor was developed using magnetic graphene nanosheet (Tang et al., 2011). This sensing platform was further improved by using DNase I for the signal amplification. As described in GO-based FRET aptasensor, DNase I could repeatedly digest DNA aptamer tagging redox molecule, detached from graphene electrode by the binding of targets. Thus, redox molecules were accumulated. As a result, the electrochemical signal was amplified. By the recent reports, GO seems to be the most suitable graphene material in aspect of sensitivity (Loo et al., 2012). Graphene have been also used as multi-functional nanocarrier for loading electroactive molecules, enzymes or receptors based on its large surface area (Huang et al., 2012). For instance, Yang and co-workers developed an electrochemical aptasensor for multiplexed detection for PDGF and thrombin (Bai et al., 2012). In this method, graphenes were conjugated with two different redox molecules and secondary aptamers individually, and they were used as reporters to enhance sensitivity in sandwich binding based electrochemical aptasensor.

2.5.3. Silica nanoparticles

Since the report of synthesis of mono-dispersed silica nanoparticles (SiNPs) by Stober and their co-workers in 1968, SiNPs have been broadly used in various areas (Stober et al., 1968). Especially, variety of dyes can be easily encapsulated inside the SiNPs uniformly, in which photo-bleaching is minimized and the dye is protected from outside environments *i.e.* oxidation or degradation conditions. In addition, dye-doped SiNPs require no further signal amplification because thousands of dye molecules are already existed inside single particle. These advantages of dye-doped SiNPs attract researchers to use them in biosensor development (Lian et al., 2004).

Several detection methods have been developed using dye-doped SiNPs. Wang and co-workers described that $Ru(bby)_3^{2+}$-doped SiNPs was used as reporter in aptasensor. Dye-doped SiNPs were conjugated with anti-thrombin aptamers. Then, a thrombin was detected based on target induced displacement format (Wang and Liu, 2009). Recently, Babu developed an aptasensors for thrombin detection using [Ru(dpsphen)3]4-(dpsphen-4,7-diphenyl-phenanthroline disulfonate) ion encapsulated SiNPs. Dye-doped SiNPs were conjugated with anti-thrombin aptamers by covalent binding via 5′ end of aptamers, these aptamers were also modified with a DABCYL quencher at 3′ end. The structure of anti-thrombin aptamers transited to G-quadruplex form by the binding with thrombin in which the DABCYL closed to SiNPs, consequently the luminescence signal reduced reverse proportional to thrombin concentration. Dye-doped SiNPs have been applied frequently in biosensors, but polymer-based fluorescence particles are more successively applied in commercial products for multiplexed fluorescence assay such as Luminex bead assay (Life Technologies, USA).

SiNPs can be also used as solid support for separation, not reporter (Babu et al., 2013). Cai et al. reported ATP detection assay using ATP binding aptamers and SiNPs (Cai et al., 2011). They designed the complementary sequences against an ATP binding aptamer and immobilized them on the SiNPs. In the presence of ATP, aptamers did not form a double-helix structure due to the interaction with ATP, subsequently they were displaced from complementary DNA immobilized on SiNPs. Then, the concentration of ATP was quantified by the addition of chelating dye (Hoechst33258) which preferentially intercalate at AT-rich region of double stranded DNA. SiNPs can be easily separated by centrifugation. Although this assay composed multiple steps, but this target induced displacement approach using chelating dye is applicable to other aptamers with low cost. A sandwich assay using aptamers and SiNPs was also demonstrated for the sensitive and selective detection of thrombin and lysosome in biological media (Wang and Liu, 2009). In this system, the capturing aptamers were immobilized on SiNPs and secondary aptamers were labeled with fluorescein. Dye-labeled aptamers were assembled on SiNPs via sandwich binding in the presence of targets. Additionally the signal was amplified to 1.06 nM of LOD by coupling the cationic conjugated polymer that enhanced the fluorescence signal by energy transfer from polymer to fluorescein. An application of SiNPs to separation and concentration is very simple and convenient via centrifugation, but magnetic particles are more suitable in automation as a separation module in system.

SiNPs can contain multiple dyes in single particle, which enable to produce the numerous SiNPs emitting different fluorescence by combination of various dyes, respectively. These multiple dye-doped SiNPs have been used multiplex detection system. For instance, multiplexed cancer cell detection was accomplished by the combination of three different aptamers and dye-doped SiNPs (Chen et al., 2009b). First SiNPs encapsulated just FAM molecules, and second SiNPs contained both of FAM and R6G dyes. Third SiNPs employed all of FAM, R6G, and ROX inside single nanoparticle. The excitation and emission wavelength of these dyes were rather overlapped. So, a fluorescence resonance energy transfer (FRET) was occurred among three dyes inside SiNPs. In

this system, a single wavelength of excitation could produce the three different wavelength of emission, which simplified the optics in the detection modules.

2.6. Nanocrystal quantum dot-based aptasensors

Quantum dots (QDs) are semiconducting nanocrystals. They offer some advantages compared to organic fluorescent dyes such as lower photobleaching, longer lifetime, greater fluorescence intensity, and sharper emission bands. In addition, various QDs showing different emission wavelengths can be excited at same wavelength due to the broad absorption, which is very favorable to construct fluorescent resonance energy transfer (FRET) assay (Zhou, 2012). Based on these advantages, QDs have been actively studied in biosensor applications including aptasensors.

Ellington's group proposed a FRET-based aptasensor for the detection of proteins (Levy et al., 2005). In this study, authors functionalized QDs with thrombin binding aptamers and prepared quencher-labeled oligonucleotides that can hybridize with thrombin binding aptamer. In the absence of thrombin, the fluorescence of QDs was quenched by close proximity with quencher by the hybridization between aptamers and its complementary sequences. In the presence of thrombin, the hybridization was destroyed by the interaction between aptamers and targets. Consequently, the fluorescence signal of QDs was recovered proportional to target concentration. Based on same approach, a fluorescence dye-modified complementary DNA to aptamer was successfully applied to FRET-based aptasensors for cocaine detection (Zhang and Johnson, 2009). Here, cocaine aptamer conjugated QDs and Cy5-modified complementary DNA were prepared. Cy5 was closed to QDs by the hybridization between cocaine aptamer and its complementary DNA in the absence of cocaine, caused the excitation of Cy5 by QDs. Cocaine addiction led the dissociation of Cy5-modified complemented DNA from the aptamers on QDs. Thus, a fluorescence signal of Cy5 was reduced in reversely proportion to the cocaine concentration. This strategy was also applied in FRET-based aptasensor using the intercalating dyes and non-modified oligonucleotides, not using dye-modified complementary DNA. Here, the intercalating dyes were incorporated in the double-helix structure of aptamer-complementary DNA. Thus, the fluorescence of QDs was quenched by close proximity of intercalating dyes in the absence of targets. The fluorescence of QDs was recovered by the addition of targets. This is more profitable to develop the aptasensors in aspect of manufacturing cost. QDs are considerably expensive materials, compared to other fluorescence dyes or particles. However, the price of QDs has recently been continuously decreasing, because they are intensively applied in the display products such as QD-LED display. Therefore, QDs are expected to be more widely applied in biosensors in near future.

The conformational change of aptamers depending on the presence of target has been utilized to develop the FRET-based aptasensor using QDs. Chen and co-workers prepared the thrombin aptamer conjugated QDs (Chi et al., 2011). In the absence of target, the thrombin aptamer possessed a stem-loop structure. The fluorescence dye BOBO-3 was intercalated into this duplex stem region of aptamer; thus, the fluorescence dye was excited by the emitted light from QDs. The conformation of thrombin aptamer was transited into G-quadruplex structure by the binding to thrombin, which did not allow the intercalation of the fluorescence dye into the aptamers. Consequently, a fluorescence signal of BOBO-3 was reduced according to increasing thrombin concentration.

One of the important reasons why researchers are interested in QDs is because of their utility in multiplexing biosensors. QDs have a broad excitation wavelength and narrow emission band that is very favorable to construct multiplexing fluorescence biosensors. For example, Lu's group reported a multiplex aptasensor using QDs for the simultaneous detection of cocaine and adenosine (Liu et al., 2007b). In this study, two kinds of QDs having different emission wavelengths (525 nm, 585 nm) and AuNPs were used as reporter and quencher, respectively. AuNPs and QDs were functionalized with two DNA probes that were partially complemented to part of aptamers, respectively. In the absence of targets, AuNPs and QDs were assembled by sandwich hybridization between DNA probes on nanoparticles and aptamers, resulting in the quenching of fluorescence signal of QDs by AuNPs. The addition of targets caused the dissociation of hybridization and resulted in increasing fluorescence signal of QDs. Both of adenosine and cocaine targets were simultaneously detected in one pot assay. Although the color change of the solution could also be observed upon the aggregation and dispersion of AuNPs in the absence and presence of targets, but the distinguishable observation for multiple targets was not possible in this colorimetric assay. Kim and Jurng also proposed a homogeneous fluorescence aptasensor for multiplex detection using AuNPs and three kinds of QDs (Kim and Jurng, 2011). The authors prepared three kinds of aptamer/QD conjugates and attached them on the surface of unmodified AuNPs by electrostatic interaction. Consequently, the fluorescence of all QDs was effectively quenched by AuNPs. By the addition of targets (mercury ion, potassium ion and adenosine), aptamers were displaced from AuNPs by the binding to target, resulting in recovering of fluorescence signal at corresponding wavelength to aptamer/QDs pairs. All of the three targets could also be simultaneously detected under single excitation wavelength in this system. This assay is a very simple multiplexing method, thus it's proper for on-site application. However, the interaction between QD-aptamer conjugates and AuNPs still seems to be not well controlled accordingly leading to a not sufficient coefficient of variation.

Lin and co-workers demonstrated another application of QDs in electrochemical aptasensor (Ding et al., 2010a). Here, AuNPs were conjugated aptamers and QDs (CdS) and an electrode was modified with capture aptamers. In the presence of target, AuNP/QDs complexes were localized on the electrode by sandwich binding. After washing step, QDs were degraded by the treatment of acidic reagent, subsequently the concentration of Cd^{2+} was measured by voltammetric analysis. Since QDs composed of large amount of Cd^{2+}, this aptasensor showed an ultrasensitive analytical performance (0.55 fM, LOD) and successively applied to detect thrombin in clinical serum samples. This system should be very suitable with its excellent sensitivity and simplicity for commercialization if the acidic treatment of QDs can be well controlled with high reproducibility. This assay can also be applied for multiplex detection by using several QDs materials composed of various elements.

3. Surface plasmon resonance (SPR)-based aptasensors

To date, a number of aptasensors have been developed based on remarkable merits over immunoassay. Among the different available aptasensing platforms, SPR hold a great promise for the development of aptasensors, because this technology offers label-free detection and real time quantitative analysis, and provides binding constant determination. SPR is a mass-sensitive biosensor which sensitively detects mass changes associated with the change in refractive index at the surface due to the molecular surface binding events. SPR-based biosensors have been used for almost three decades, since this technology was firstly demonstrated by Leidberg et al. in 1983. The technology provides the opportunity to develop an optimized protocol for ssDNA conjugation on SPR gold film by simple avidin–biotin basis, and demonstrate the first DNA–DNA hybridization analysis in real time,

detected using SPR platform (Wood, 1993). SPR promotes the adoption of aptamers as versatile molecular probe for SPR biosensor generation and signal amplification development. Currently, there are two main principles to be considered to generate SPR signal amplifications. 1) The substrate enhancement using nanomaterials such as graphene oxide (Singh et al., 2015), Au/Ag (Hao et al., 2011) and nanodots (Kravets et al., 2013) coated metallic thin films as the reaction surface, and 2) the use of amplification tags such as nanomaterials (plasmonic nanoparticles, magnetic nanoparticles and nanocrystal) and enzymes. To this concern, the first principle is getting rapidly focused to create comfortably sensitive SPR film for POCT device, in parallel to the second principle, which therefore pointing out the usefulness of aptamers to not only serve as target capturing probe (as can be easily modified to wide range of film materials), but also as amplification tag-modified probe for signal generation.

Previously, SPR-based aptasensor for proteins are well established and widely used to detect various proteins such as tubulin (Fukusaki et al., 2001), thrombin and thyroid transcription factor 1 (Murphy et al., 2003), HIV-1 Tat protein (Tombelli et al., 2005), C-reactive protein (Bini et al., 2008), human immunoglobulin E (IgE) (Kim et al., 2009a) and adipokines (Lee et al., 2008; Park et al., 2012), by a single-site binding configuration. Concerning to the signal amplification issue, the two-site binding configuration was adopted that combined the aptamers and antibodies binding to a specific target. In this case, an enzymatically amplified SPR imaging (SPRi) assay was introduced to produce higher detection of thrombin and VEGF proteins (Li et al., 2007). This study used HRP-conjugated antibody acted as signaling probe, while aptamer was conjugated on SPR gold chip to capture target proteins. In the presence of HRP substrate, precipitates was formed on the SPR sensor surface, producing amplified SPRi signal, thus highly increased the sensitive detection of thrombin and VEGF with LOD 1 pM and 500 fM, respectively. Next, AuNPs were combined with SPR aptasensors to enhance the detection of human IgE, which produced the lowest LOD of human IgE (1 ng/ml) (Wang et al., 2009b), compared to the previous report without using AuNPs labeled aptamer (Kim et al., 2009a).

Besides proteins, SPR aptasensors for small molecules detection has gained interest since the SPR signal amplification strategies are rapidly investigated. This is because, without signal amplification approach, SPR based detection of small molecules was hardly accomplished due to a low change of refractive index produced by low molecular mass. Wang and co-worker initiated adenosine detection by SPR aptasensor using AuNPs amplification signal method based on surface inhibition detection (Wang and Zhou, 2008). In this study, adenosine aptamers were firstly conjugated on SPR gold film and hybridized with its complementary DNA-tagged AuNPs, producing high SPR responses. In the presence of adenosine, adenosine aptamers changed to the tertiary structure upon binding to adenosine, preventing the hybridization of aptamers to their complementary DNA-tagged AuNPs, thus highly reduced the SPR response unit. Latest SPR aptasensing approach for adenosine detection was enhanced by Qiu's group, which combined both amplification approaches of using AuNPs conjugation and DNA strand displacement cycle (Yao et al., 2015a). The detection limit was improved down to 0.21 pM, which is 3 orders of magnitude enhanced, compared to the used of each amplification approach, separately (Wang et al., 2009c). To date, the best LOD for adenosine was reported by the same group where they applied both above mentioned SPR signal amplification principles, by using aptamer-based target-triggering cascade multiple cycle amplification (for tag modification) and streptavidin-coated AuNPs (AuNPs-SA) enhancement (for SPR film enhancement) to enhance the SPR signal with adenosine LOD of 4 fM (Yao et al., 2015b).

Overall, various signal amplification methods reported were shown to rely on the sandwich-type detection basis. Accordingly, dual aptamers which can be tuned into both capturing and tag-modified probe for detecting their binding target are more indispensable to substitute expensive yet complicated sandwich-based biosensor ligands. For example, aptamer-based rolling circle amplification (RCA) technique was combined with AuNPs-labeled probes to detect thrombin down to 1 aM LOD (He et al., 2014). In this study, the secondary aptamer for thrombin was modified to link with primer region for RCA reaction and as a template for padlock probe ligation. These amplified sequences were then bound to the immobilized thrombin, which was initially captured by primary aptamer on SPR chip. Thus, AuNPs-labeled probes were assembled on the RCA products to further amplify the SPR signal. Most recently, simpler SPR signal enhancement was achieved for thrombin detection using core-shell gold capped magnetic nanoparticles (GMPs) conjugated with thrombin secondary aptamer, resulted in the LOD as low as 0.1 nM (Chen et al., 2015). Moreover, Gu's research group has demonstrated ultrasensitive detection of visceral adipose tissue derived serpin (Vaspin) and even to virus target, the bovine viral diarrhea virus type 1 (BVDV type 1), in which the AuNPs functionalized with thiol-modified secondary aptamers were used as the SPR amplification probe, thus resulting in LOD down to 3.5 ng/ml for Vaspin (Ahmad Raston and Gu, 2015) and 800 copies/ml for BVDV type 1 detection (Park et. al., 2014). This effectively simple approach, however, has limitation due to only small numbers of dual aptamers available to date. Thus, the development of dual aptamers for more target of interest should be well focused and given serious attention.

It is true that all the above-mentioned SPR-based aptasensors were carried out with laboratory instruments and required trained personnel. To this concern, a membrane-based microfluidic device integrated with SPR sensor was introduced to provide an easier sample handling and cost effective analysis (Chuang et al., 2014). This disposable device was designed to have systematic fluid flow for each step of washing, detection, and signal amplification. Initially, the washing solution was deposited into the transport membrane to wet the rayon membrane. Next, sample solution was flown through the detection region, and contained in the transport membrane. Then, a controlled concentration of streptavidin was added to amplify the SPR signal. Washing step was then carried out to remove unbound sample and streptavidin. Overall detection process could be done within 30 min, with a LOD of 10 pM achieved for Interferon gamma (IFN-γ).

Furthermore, the practical applications of aptasensors or aptamer-based diagnostics are still feeble and there is no successive product in market. Therefore, more intensive efforts for successive commercial applications of aptasensors are required to overcome the huddle of immunoassay and root aptasensor in bioanalytical industry. In aspect of this, a lateral flow strip might be an appropriate platform because a manufacturing process is well established with low cost and it is very user-friendly. Aptamers have some inherent advantages over antibodies in commercial aspect as well as technical advantages as the following: 1) Aptasensors do not require a sophisticated temperature control for storage and distribution. Aptamers can recover their activity upon hydration with minimum performance loss. Especially, this is one of the major limitations for the application of POCT in developing countries because the temperature control system raises the selling price of products. 2) The production of aptamers by chemical synthesis supports less lot-to-lot variation, simple quantification and quality check, and price competitiveness compared to the production of antibodies. 3) Aptamers are more favorable for well-oriented immobilization on strip or nanomaterials like AuNPs, and a loading amount is also higher than antibodies due to their small size. 4) Aptasensors can be reused by simple thermal or chemical treatment if necessary. 5) Finally, as abovementioned, no

limitation to analytes including small molecules and even metal ions is also important to expand the markets of aptasensors in clinical diagnostics (metabolites or neurotransmitter), environment monitoring (toxic compounds), food safety (antibiotics), and anti-terrorism (chemical warfare agents).

4. Lateral flow strip-based aptasensors

A lateral flow strip aptasensor can be developed by two approaches, sandwich format and target induced conformational change/displacement format that were described enough in above sections. In this section, the recent examples and advances of lateral flow strip aptasensors were introduced and the strategies for the design of them were comprehended. Xu and co-workers demonstrated a lateral flow aptasensor for thrombin detection according to the conventional sandwich format (Xu et al., 2009a). Here, biotinylated capture aptamers were immobilized on the test line via avidin–biotin interaction, and secondary aptamer functionalized AuNPs were loaded on the conjugated pad. When the sample containing thrombin was loaded on sample pad, thrombin migrated along the strip by capillary action and bound to aptamer functionalized AuNPs on conjugation pad. Subsequently, the complex of thrombin/aptamer-AuNPs continually migrated along the strip and they were recognized by capture aptamers immobilized. As a result, the red line was observed due to the accumulation of AuNPs in the test line. The excess aptamer functionalized AuNPs passed through the test line and captured by complemented DNA probes in control zone. Thus, a second red line was observed in control zone. For the quantitative detection of thrombin, a strip reader was used and resulted a linear calibration curve in a range of 5–100 nM, which was similar to the sensitivity of antibody based lateral flow immunoassay for same target. This lateral flow strip aptasensor was expanded to the detection of Ramos cell (Liu et al., 2009b). This aptasensor could detect as low as 4000 Ramos cells by visual observation and 800 Ramos cells with a portable strip reader within 15 min. In normal lateral flow strip aptasensors, the formation of red line on control zone was not rather reliable because the residence time of aptamer-AuNP conjugates on control was not enough for hybridization. The strategy of Bruno using dual labeled aptamer provided one way to overcome this problem (Bruno 2014). Authors prepared aptamers modified with biotin and digoxigenin at 5′ and 3′ ends in each. And the modified aptamers conjugated to streptavidin coated AuNPs via avidin–biotin interaction. In addition, anti-digoxigenin antibodies were immobilized on control zone. Under these modifications of assay, a reliable and strong red line on control zone could be obtained. This sandwich-type assay-based lateral flow strip aptasensors seems to be most close to commercial product if dual aptamers for a single target are available.

Xu and co-workers developed a lateral flow aptasensor based on the target induced displacement of aptamer for small molecular target (ochratoxin) that is not available to sandwich binding due to small size (Wang et al., 2011). In this method, polyA tail tagged aptamers were conjugated to AuNPs and complementary DNAs to aptamer were immobilized on the test zone. In the presence of target, aptamer–AuNP conjugates were not captured by complemented DNA and passed through test zone, following captured on control zone on where polyT oligonucleotides were immobilized. In the absence of target, aptamer-AuNP conjugates were captured on test zone by hybridization between aptamers and complementary DNA, resulting in the observation of red line on test zone. The LOD of this lateral flow aptasensor was 1 ng/ml by visual observation that was lower than one of lateral flow antibody strip. As another approach, from the illustrated Fig. 6, Lu and co-workers applied a strategy of AuNP networking in lateral flow aptasensor for adenosine detection (Liu et al., 2006). As described in the section of colorimetric aptasensor, AuNPs functionalized with two different partially complementary DNA (cDNA) probes and biotin were linked as network by the hybridization of two cDNA probes to aptamers. In the presence of adenosine, biotin tag on AuNPs was hindered by networked AuNPs, thus AuNPs were passed through test zone where streptavidin was immobilized. In the presence of adenosine, biotin was open by the dispersion of AuNPs, resulting in observation of red line on test zone by capturing of AuNPs via avidin–biotin interaction. This method inherently has same problem with sandwich format in the hybridization efficiency between aptamers and complemented DNA probes on test zone. To overcome this issue, the dipstick platform have been adopted in lateral flow aptasensors, which possessed two steps, pre-reaction and dipping a dipstick (Shim et al., 2014). In this method, aptamer was modified with biotin and complementary DNA (cDNA) was labeled with Cy5 dye. The competitive interaction between complemented DNA and target in sample to aptamer was occurred during pre-reaction. Subsequently, a dipstick was dipped into the mixture. In the absence of

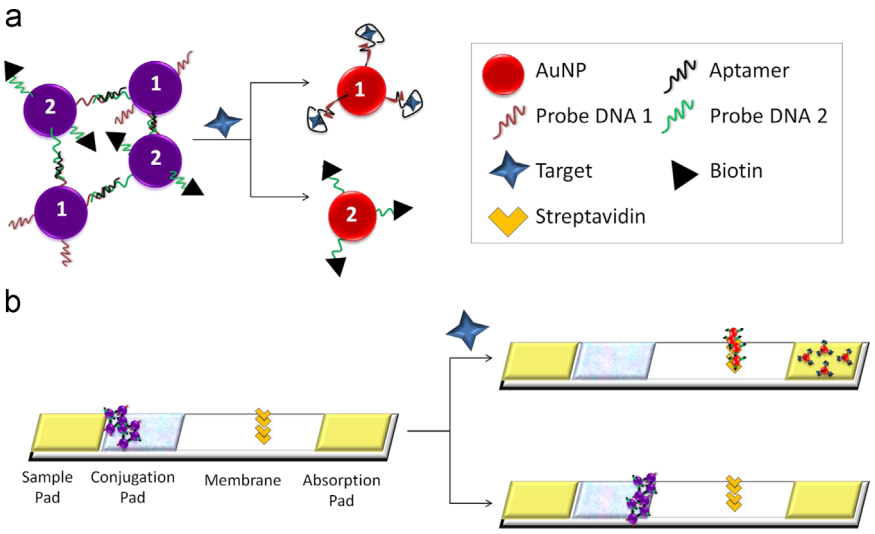

Fig. 6. Lateral flow strip platform-based aptasensor. (a) Target –induced disassembly of AuNPs aggregates into red-colored dispersed AuNPs; (b) Lateral flow devices loaded with the aggregates on the conjugation pad and streptavidin on the strip membrane. (For interpretation of the references to color in this figure legend,the reader is referred to the web version of this article.)

Table 2
Surface plasmon resonance (SPR) and lateral flow strip-based aptasensors.

Platform	Target	LOD	Method	Signal amplification	Reference
SPR	Tubulin	ND[a]	Simple binding	–	(Fukusaki et al., 2001)
SPR	Thrombin Thyroid transcription factor 1	ND	Simple binding	–	(Murphy et al., 2003)
SPR	HIV-1 Tat protein	0.12 ppm	Simple binding	–	(Tombelli et al., 2005)
SPR	C-reactive protein	0.005 ppm	Simple binding	–	(Bini et al., 2008)
SPR	Human IgE	141 ng/ml	Simple binding	Liposome	(Kim et al., 2009a)
SPR	Retinol binding protein 4 (RBP4)	1.58 μg/ ml	Simple binding	–	(Lee et al., 2008)
SPR	Nampt	ND	Simple binding	–	(Park et al., 2012)
SPR	Thrombin VEGF	1 pM (thrombin) 500 fM (VEGF)	Sandwich	HRP-conjugated	(Li et al., 2007)
SPR	Human IgE	1 ng/ml	Sandwich	AuNPs	(Wang et al., 2009b)
SPR	Human IgE	2.07 ng/ml	Sandwich	Antibody	(Kim et al., 2009a)
SPR	Adenosine	1 nM	TICC[b]	AuNPs	(Wang and Zhou, 2008)
SPR	Adenosine	0.21 pM	TID[c]	AuNPs and DNA strand displacement cycle	Yao et al., 2015a)
SPR	Adenosine	10 nM	TICC	AuNPs	(Wang et al., 2009c)
SPR	Adenosine	4 fM	TID	Cascade multiple cycle amplification and streptavidin-coated AuNPs chip	(Yao et al., 2015b)
SPR	Thrombin	1 aM	Sandwich dual aptamers	Rolling circle amplification (RCA) technique and AuNPs-labeled probes	(He et al., 2014)
SPR	Thrombin	0.1 nM	Sandwich dual aptamers	Core–shell gold capped magnetic nanoparticles (GMPs)	(Chen et al., 2015)
SPR	Vaspin	3.5 ng/ml	Sandwich dual aptamers	AuNPs	(Ahmad Raston and Gu, 2015)
SPR	BVDV type 1 virus	800 copies/ml	Sandwich dual aptamers	AuNPs	(Park et al., 2014)
SPR	IFN-γ	10 pM	Simple binding	Membrane-based microfluidic disposable device	(Chuang et al., 2014)
Strip	Thrombin	5 nM	Sandwich dual aptamers	AuNPs	(Xu et al., 2009a)
Lateral flow strip	Ramos cell	4000 cells (visual observation) 800 cells (portable strip reader)	Sandwich dual aptamers	AuNPs	(Liu et al., 2009b).
Lateral flow strip	*E. coli*	3000 cells (using AuNPs) 300 cells (using Qds)	Sandwich dual aptamers	AuNPs and Qds	(Bruno, 2014)
Lateral flow strip	Ochratoxin	1 ng/ml	TID	AuNPs	(Wang et al., 2011)
Lateral flow strip	Adenosine	20 μM (Adenosine) 10 μM (Cocaine)	TID	AuNPs	(Liu et al., 2006).
Lateral flow strip	Aflatoxin B1	0.1 ng/ml	TICC	Cy5 dye	(Shim et al., 2014)

[a] ND not determined.
[b] TICC target-induced conformation change of aptamer.
[c] TID target-induced displacement of aptamer/DNA probe.

target in sample, duplex DNAs of aptamer/cDNA tagging both of biotin and Cy5 at each end were captured by streptavidin immobilized on test zone thus a fluorescence signal on test zone could be observed. In the presence of target in sample, duplex DNA of aptamer/cDNA was not formed due to the binding of aptamers to targets during pre-reaction. Consequently, fluorescence signal on test zone was not observed because only aptamer was captured by streptavidin on test zone. This dipstick platform of aptasensor could detect aflatoxin B1 as low as 0.1 ng/ml in the buffer. A lateral flow strip aptasensor based-on target induced displacement is not convenient and also time consuming, compared to sandwich-based lateral flow strip assay, but it might be very powerful for a simple on-site detection of small molecules which are not available for dual aptamer isolation inherently. The SPR-based aptasensors and lateral flow strip-based aptasensors discussed in this review were summarized in Table 2.

5. Conclusions and perspectives

In a past decade, the development of aptasensors have been remarkable and aptasensors have enough demonstrated their merits and potentials in bio-analysis field. Despite of this excellent progress, the market of aptasensors and aptamer-based diagnostics is not explored yet. For the successive penetration of aptasensors into market, a number of issues should be solved at technical and industrial aspects. At first, only a few of aptamers such as thrombin, adenosine, cocaine, ATP and PDGF binding aptamer have been utilized in numerous aptasensors as proof of concepts and principles of novel aptamer-based sensors due to their well understanding and characterization. For commercial application, however, researchers have to target analytes that have a need of end-user to be detected in market. Especially, it is very difficult to alter the immune-sensors, which were already approved for clinical test due to regulatory issues, although aptasensors have some merits over immune-sensors for same targets and purposes. Therefore, the development of aptasensors for newly emerged targets might be good approach to compete with immune-sensors for commercialization. Of course, high quality aptamers for commercially important targets should be isolated in advance of aptasensor development. Secondly, almost aptamer-based sensing methods reported so far is a little sophisticated or complicated to operate as a sensor, which normally raises a coefficient of variation and is not user-friendly in field. Therefore, it is important that various aptasensors should be coupled in practically feasible sensor platforms such as lateral flow strip. The sensitivity of POC type aptasensors should also be more improved as well as specificity through powerful signal amplification methods or enhancing affinity of aptamers to target. The incorporation of nanomaterials such as AuNPs to aptasensors can realize the excellent improvement of sensitivity. To compete with well-established immuno-sensors or enzyme-based biosensors, a few successful examples need to demonstrate a potential of commercial application of aptasensors and facilitate their commercialization. The realization in making aptasensors successfully is now possible, since a successive development of cognate aptamer duos, obtained from the immobilization-free method using graphene oxide, which allow the use of sandwich-type assays possible.

The global market for aptamers and aptasensors is also expected to grow rapidly, backed by technical advancements with respect to selection process, synthesis of aptamers and analytical performance of aptasensors. In addition, aptamer companies in bio-analytical and pharmaceutical industry have been founded continuously. As the report of 'Markets and Markets', the global market size of aptamer was $287 M in 2013, and is anticipated to reach about $2.1 B by 2018 with 49.24% CAGR (compound annual growth rate). Especially, the global market for aptasensors and aptamer-based diagnostics was about $45.2 M in 2013, and is expected to attain to approximately $467 M by 2018 with 59.6% CAGR. Although the most of this market is built with aptamer synthesis and aptamer isolation service, there is no doubt that aptamers and aptasensors will be more spotlighted in future. Aptasensors are now starting to demonstrate their worth as a rival of traditional immunoassay in biosensor industry.

Acknowledgment

This work was supported by the National Research Foundation of Korea (NRF) Grant funded by the Korea Government (MEST) (no. 2013R1A1A2021531).

References

Ahmad Raston, N.H., Gu, M.B., 2015. Biosens. Bioelectron. 70, 261–267.
Ajayan, P.M., 1999. Chem. Rev. 99, 1787–1799.
Babu, E., Mareeswaran, P.M., Rajagopal, S., 2013. J. Fluoresc. 23, 137–146.
Bai, L.J., Yuan, R., Chai, Y.Q., Zhuo, Y., Yuan, Y.L., Wang, Y., 2012. Biomaterials 33, 1090–1096.
Baker, B.R., Lai, R.Y., Wood, M.S., Doctor, E.H., Heeger, A.J., Plaxco, K.W., 2006. J. Am. Chem. Soc. 128, 3138–3139.
Bamrungsap, S., Chen, T., Shukoor, M.I., Chen, Z., Sefah, K., Chen, Y., Tan, W.H., 2012. ACS Nano 6, 3974–3981.
Baron, R., Willner, B., Willner, I., 2007. Chem. Commun. 4, 323–332.
Bini, A., Centi, S., Tombelli, S., Minunni, M., Mascini, M., 2008. Anal. Bioanal. Chem. 390, 1077–1086.
Bruno, J.G., 2014. Pathogens 3, 341–355.
Burda, C., Chen, X., Narayanan, R., El-Sayed, M.A., 2005. Chem. Rev. 105, 1025–1102.
Cai, L., Chen, Z.Z., Dong, X.M., Tang, H.W., Pang, D.W., 2011. Biosens. Bioelectron. 29, 46–52.
Cao, X.X., Li, S.H., Chen, L.C., Ding, H.M., Xu, H., Huang, Y.P., Li, J., Liu, N.L., Cao, W.H., Zhu, Y.J., Shen, B.F., Shao, N.S., 2009. Nucleic Acids Res. 37, 4621–4628.
Castellana, E.T., Gamez, R.C., Gomez, M.E., Russell, D.H., 2010. Langmuir 26, 6066–6070.
Chang, C.C., Wei, S.C., Wu, T.H., Lee, C.H., Lin, C.W., 2013. Biosens. Bioelectron. 42, 119–123.
Chen, C., Zhao, J., Jiang, J., Yu, R., 2012a. Talanta 101, 357–361.
Chen, D., Feng, H., Li, J., 2012b. Chem. Rev. 112, 6027–6053.
Chen, H., Yu, C., Jiang, C., Zhang, S., Liu, B., Kong, J., 2009a. Chem. Commun. 33, 5006–5008.
Chen, H.X., Qi, F.J., Zhou, H., Jia, S.S., Gao, Y.M., Koh, K., Yin, Y.M., 2015. Sens. Actuators B: Chem. 212, 505–511.
Chen, L., Lee, S., Lee, M., Lim, C., Choo, J., Park, J.Y., Lee, S., Joo, S.W., Lee, K.H., Choi, Y. W., 2008. Biosens. Bioelectron. 23, 1878–1882.
Chen, X.L., Estevez, M.C., Zhu, Z., Huang, Y.F., Chen, Y., Wang, L., Tan, W.H., 2009b. Anal. Chem. 81, 7009–7014.
Chi, C.W., Lao, Y.H., Li, Y.S., Chen, L.C., 2011. Biosens. Bioelectron. 26, 3346–3352.
Cho, E.J., Lee, J.W., Ellington, A.D., 2009. Annu. Rev. Anal. Chem. 2, 241–264.
Cho, E.J., Yang, L., Levy, M., Ellington, A.D., 2005. J. Am. Chem. Soc. 127, 2022–2023.
Choi, H.K., Lee, J.H., 2013. Anal. Methods 5, 6964–6968.
Chuang, T.L., Chang, C.C., Chu-Su, Y., Wei, S.C., Zhao, X.H., Hsueh, P.R., Lin, C.W., 2014. Lab Chip 14 (16), 2968–2977.
Cruz-Aguado, J.A., Penner, G., 2008. Anal. Chem. 80, 8853–8855.
Cui, D., Pan, B., Zhang, H., Gao, F., Wu, R., Wang, J., He, R., Asahi, T., 2008. Anal. Chem. 80, 7996–8001.
Ding, C.F., Ge, Y., Lin, J.M., 2010a. Biosens. Bioelectron 25, 1290–1294.
Ding, N., Yan, N., Ren, C.L., Chen, X.G., 2010b. Anal. Chem. 82, 5897–5899.
Du, Y., Li, B., Wei, H., Wang, Y., Wang, E., 2008. Anal. Chem. 80, 5110–5117.
Du, Y., Li, B.L., Wang, F., Dong, S.J., 2009. Biosens. Bioelectron. 24, 1979–1983.
Du, Y., Li, B., Wang, E., 2010. Bioanal. Rev. 1, 187–208.
Fan, C., Wang, S., Hong, J.W., Bazan, G.C., Plaxco, K.W., Heeger, A.J., 2003. Proc. Natl. Acad. Sci. USA 100, 6297–6301.
Feng, K.J., Sun, C.H., Kang, Y., Chen, J.W., Jiang, J.H., Shen, G.L., Yu, R.Q., 2008. Electrochem. Commun. 10, 531–535.
Ferapontova, E.E., Olsen, E.M., Gothelf, K.V., 2008. J. Am. Chem. Soc. 130, 4256–4258.
Fischer, N.O., Tarasow, T.M., Tok, J.B.H., 2008. Anal. Biochem. 373, 121–128.
Frauendorf, C., Jaschke, A., 2001. Bioorg. Med. Chem. 9, 2521–2524.
Fukusaki, E., Hasunuma, T., Kajiyama, S., Okazawa, A., Itoh, T.J., Kobayashi, A., 2001. Bioorg. Med. Chem. Lett. 11, 2927–2930.
Gao, L.Z., Wu, J.M., Lyle, S., Zehr, K., Cao, L.L., Gao, D., 2008. J. Phys. Chem. C 112, 17357–17361.
Gao, L.Z., Zhuang, J., Nie, L., Zhang, J.B., Zhang, Y., Gu, N., Wang, T.H., Feng, J., Yang, D. L., Perrett, S., Yan, X., 2007. Nat. Nanotechnol. 2, 577–583.
Gigliotti, B., Sakizzie, B., Bethune, D.S., Shelby, R.M., Cha, J.N., 2006. Nano. Lett. 6,

159–164.
Gopinath, S.C., Lakshmipriya, T., Awazu, K., 2014. Biosens. Bioelectron. 51, 115–123.
Hao, P., Wu, Y., Li, F., 2011. Appl. Opt. 50, 5555–5558.
He, P., Liu, L., Qiao, W., Zhang, S., 2014. Chem. Commun. 50 (12), 1481–1484.
Herr, J.K., Smith, J.E., Medley, C.D., Shangguan, D., Tan, W., 2006. Anal. Chem. 78, 2918–2924.
Hu, R., Wen, W., Wang, Q., Xiong, H., Zhang, X., Gu, H., Wang, S., 2014. Biosens. Bioelectron. 53, 384–389.
Huang, C.C., Chiang, C.K., Lin, Z.H., Lee, K.H., Chang, H.T., 2008. Anal. Chem. 80, 1497–1504.
Huang, C.C., Chiu, S.H., Huang, Y.F., Chang, H.T., 2007. Anal. Chem. 79, 4798–4804.
Huang, C.C., Huang, Y.F., Cao, Z., Tan, W., Chang, H.T., 2005. Anal. Chem. 77, 5735–5741.
Huang, P.J.J., Kempaiah, R., Liu, J.W., 2011. J. Mater. Chem. 21, 8991–8993.
Huang, X., Qi, X.Y., Boey, F., Zhang, H., 2012. Chem. Soc. Rev. 41, 666–686.
Jeon, W., Lee, S., Manjunatha, D.H., Ban, C., 2013. Anal. Biochem. 439, 11–16.
Jung, J., Chen, L., Lee, S., Kim, S., Seong, G.H., Choo, J., Lee, E.K., Oh, C.H., Lee, S., 2007. Anal. Bioanal. Chem. 387, 2609–2615.
Jung, Y.K., Lee, T., Shin, E., Kim, B.S., 2013. Sci. Rep. 3, 3367.
Kim, Y.H., Kim, J.P., Han, S.J., Sim, S.J., 2009a. Sens. Actuators B: Chem. 139, 471–475.
Kim, Y.J., Kim, Y.S., Niazi, J.H., Gu, M.B., 2010a. Bioprocess Biosyst. Eng. 33, 31–37.
Kim, Y.S., Gu, M.B., 2014. Aptamer and enzyme biosensors. In: Scheper, T. (Ed.), Biosensors Based on Aptamers and Enzymes. Springer-Verlag, Berlin Heidelberg., New York, pp. 29–67.
Kim, Y.S., Jurng, J., 2011. Analyst 136, 3720–3724.
Kim, Y.S., Jurng, J., 2013. Sens. Actuators B: Chem. 176, 253–257.
Kim, Y.S., Kim, J.H., Kim, I.A., Lee, S.J., Gu, M.B., 2011. Biosens. Bioelectron. 26, 4058–4063.
Kim, Y.S., Kim, J.H., Kim, I.A., Lee, S.J., Jurng, J., Gu, M.B., 2010b. Biosens. Bioelectron. 26, 1644–1649.
Kim, Y.S., Niazi, J.H., Gu, M.B., 2009b. Anal. Chim. Acta 634, 250–254.
Kraemer, S., Vaught, J.D., Bock, C., Gold, L., Katilius, E., Keeney, T.R., Kim, N., Saccomano, N.A., Wilcox, S.K., Zichi, D., Sanders, G.M., 2011. PLoS One 6, e26332.
Kravets, V.G., Schedin, F., Jalil, R., Britnell, L., Gorbachev, R.V., Ansell, D., Thackray, B., Novoselov, K.S., Geim, A.K., Kabashin, A.V., Grigorenko, A.N., 2013. Nat. Mater. 12, 304–309.
Kwon, Y.S., Nguyen, V.T., Park, J.G., Gu, M.B., 2015. Anal. Chim. Acta 868, 60–66.
Lee, H.J., Kim, B.C., Kim, K.W., Kim, Y.K., Kim, J., Oh, M.K., 2009. Biosens. Bioelectron. 24, 3550–3555.
Lee, J.S., Han, M.S., Mirkin, C.A., 2007. Angew. Chem. Int. Ed. Engl. 46, 4093–4096.
Lee, S.J., Youn, B.S., Park, J.W., Niazi, J.H., Kim, Y.S., Gu, M.B., 2008. Anal. Chem. 80, 2867–2873.
Levy, M., Cater, S.F., Ellington, A.D., 2005. Chem. Bio. Chem. 6, 2163–2166.
Li, B.L., Wang, Y.L., Wei, H., Dong, S.J., 2008a. Biosens. Bioelectron. 23, 965–970.
Li, H., Rothberg, L., 2004a. Proc. Natl. Acad. Sci. USA 101, 14036–14039.
Li, H., Rothberg, L.J., 2004b. J. Am. Chem. Soc. 126, 10958–10961.
Li, M., Zhou, X.J., Ding, W.Q., Guo, S.W., Wu, N.Q., 2013. Biosens. Bioelectron. 41, 889–893.
Li, X.X., Qi, H.L., Shen, L.H., Gao, Q., Zhang, C.X., 2008b. Electroanalysis 20, 1475–1482.
Li, Y., Lee, H.J., Corn, R.M., 2007. Anal. Chem. 79, 1082–1088.
Lian, W., Litherland, S.A., Badrane, H., Tan, W.H., Wu, D.H., Baker, H.V., Gulig, P.A., Lim, D.V., Jin, S.G., 2004. Anal. Biochem. 334, 135–144.
Lin, Y.W., Liu, C.W., Chang, H.T., 2009. Anal. Methods 1, 14–24.
Liu, C.W., Hsieh, Y.T., Huang, C.C., Lin, Z.H., Chang, H.T., 2008. Chem. Commun. 19, 2242–2244.
Liu, C.W., Huang, C.C., Chang, H.T., 2009a. Anal. Chem. 81, 2383–2387.
Liu, G., Mao, X., Phillips, J.A., Xu, H., Tan, W., Zeng, L., 2009b. Anal. Chem. 81, 10013–10018.
Liu, J., Guan, Z., Lv, Z., Jiang, X., Yang, S., Chen, A., 2014. Biosens. Bioelectron. 52, 265–270.
Liu, J., Lee, J.H., Lu, Y., 2007a. Anal. Chem. 79, 4120–4125.
Liu, J., Lu, Y., 2006. Nat. Protoc. 1, 246–252.
Liu, J., Mazumdar, D., Lu, Y., 2006. Angew. Chem. Int. Ed. Engl. 45, 7955–7959.
Liu, J.W., Lee, J.H., Lu, Y., 2007b. Anal. Chem. 79, 4120–4125.
Liu, M., Song, J., Shuang, S., Dong, C., Brennan, J.D., Li, Y., 2014b. ACS Nano 8 (6), 5564–5573.
Liu, Z., Chen, S., Liu, B., Wu, J., Zhou, Y., He, L., Ding, J., Liu, J., 2014c. Anal. Chem. 86 (24), 12229–12235.
Loo, A.H., Bonanni, A., Pumera, M., 2012. Nanoscale 4, 143–147.
Lu, C.H., Li, J., Lin, M.H., Wang, Y.W., Yang, H.H., Chen, X., Chen, G.N., 2010. Angew. Chem. Int. Ed. Engl. 49, 8454–8457.
Lu, Y., Li, X., Zhang, L., Yu, P., Su, L., Mao, L., 2008. Anal. Chem. 80, 1883–1890.
Lu, Y., Liu, J., 2007. Acc. Chem. Res. 40, 315–323.
Ma, Z., Ding, T., 2009. Nanoscale Res. Lett. 4, 1236–1240.
Maehashi, K., Katsura, T., Kerman, K., Takamura, Y., Matsumoto, K., Tamiya, E., 2007. Anal. Chem. 79, 782–787.
Medley, C.D., Smith, J.E., Tang, Z., Wu, Y., Bamrungsap, S., Tan, W., 2008. Anal. Chem. 80, 1067–1072.
Mirkin, C.A., Letsinger, R.L., Mucic, R.C., Storhoff, J.J., 1996. Nature 382, 607–609.
Murphy, M.B., Fuller, S.T., Richardson, P.M., Doyle, S.A., 2003. Nucleic Acids Res. 31, 18.
Nguyen, V.T., Kwon, Y.S., Kim, J.H., Gu, M.B., 2014. Chem. Commun. 50, 10513–10516.
Nikoobakht, B., Wang, J.P., El-Sayed, M.A., 2002. Chem. Phys. Lett. 366, 17–23.
Nutiu, R., Li, Y., 2003. J. Am. Chem. Soc. 125, 4771–4778.
Ono, A., Torigoe, H., Tanaka, Y., Okamoto, I., 2011. Chem. Soc. Rev. 40, 5855–5866.
Ozaki, H., Nishihira, A., Wakabayashi, M., Kuwahara, M., Sawai, H., 2006. Bioorg. Med. Chem. Lett. 16, 4381–4384.
Park, J.W., Lee, S.J., Choi, E.J., Kim, J., Song, J.Y., Gu, M.B., 2014. Biosens. Bioelectron. 51, 324–329.
Park, J.W., Tatavarty, R., Kim, D.W., Jung, H.T., Gu, M.B., 2012. Chem. Commun. 48, 2071–2073.
Park, K.S., Kim, M.I., Cho, D.Y., Park, H.G., 2011. Small 7, 1521–1525.
Pavlov, V., Xiao, Y., Shlyahovsky, B., Willner, I., 2004. J. Am. Chem. Soc. 126, 11768–11769.
Ping, J., Zhou, Y., Wu, Y., Papper, V., Boujday, S., Marks, R.S., Steele, T.W., 2015. Biosens. Bioelectron. 64, 373–385.
Pu, W.D., Zhang, L., Huang, C.Z., 2012. Anal. Methods 4, 1662–1666.
Radi, A.E., Sanchez, J.L.A., Baldrich, E., O'Sullivan, C.K., 2005. Anal. Chem. 77, 6320–6323.
Ravalli, A., Rivas, L., de la Escosura-Munz, A., Pons, J., Merkoci, A., Marrazza, G., 2015. J. Nanosci. Nanotechnol. 15, 3411–3416.
Rodriguez, M.C., Kawde, A.N., Wang, J., 2005. Chem. Commun. 34, 4267–4269.
Sharon, E., Freeman, R., Tel-Vered, R., Willner, I., 2009. Electroanalysis 21, 1291–1296.
Shen, L., Chen, Z., Li, Y.H., Jing, P., Xie, S.B., He, S.L., He, P.L., Shao, Y.H., 2007. Chem. Commun. 21, 2169–2171.
Shi, Y., Dai, H.C., Sun, Y.J., Hu, J.T., Ni, P.J., Li, Z., 2013. Analyst 138, 7152–7156.
Shim, W.B., Kim, M.J., Mun, H., Kim, M.G., 2014. Biosens. Bioelectron. 62, 288–294.
Singh, M., Holzinger, M., Tabrizian, M., Winters, S., Berner, N.C., Cosnier, S., Duesberg, G.S., 2015. J. Am. Chem. Soc. 137, 2800–2803.
Smith, J.E., Medley, C.D., Tang, Z., Shangguan, D., Lofton, C., Tan, W., 2007. Anal. Chem. 79, 3075–3082.
So, H.M., Park, D.W., Jeon, E.K., Kim, Y.H., Kim, B.S., Lee, C.K., Choi, S.Y., Kim, S.C., Chang, H., Lee, J.O., 2008. Small 4, 197–201.
So, H.M., Won, K., Kim, Y.H., Kim, B.K., Ryu, B.H., Na, P.S., Kim, H., Lee, J.O., 2005. J. Am. Chem. Soc. 127, 11906–11907.
Song, Y., Zhao, C., Ren, J., Qu, X., 2009. Chem. Commun. 15, 1975–1977.
Song, Y.H., Yang, X., Li, Z.Q., Zhao, Y.J., Fan, A.P., 2014. Biosens. Bioelectron. 51, 232–237.
Sreeprasad, T.S., Samal, A.K., Pradeep, T., 2008. Langmuir 24, 4589–4599.
Stewart, M.E., Anderton, C.R., Thompson, L.B., Maria, J., Gray, S.K., Rogers, J.A., Nuzzo, R.G., 2008. Chem. Rev. 108, 494–521.
Stober, W., Fink, A., Bohn, E., 1968. J. Colloid Interface Sci. 26, 62–69.
Stojanovic, M.N., de Prada, P., Landry, D.W., 2001. J. Am. Chem. Soc. 123, 4928–4931.
Subramanian, P., Lesniewski, A., Kaminska, I., Vlandas, A., Vasilescu, A., Niedziolka-Jonsson, J., Pichonat, E., Happy, H., Boukherroub, R., Szunerits, S., 2013. Biosens. Bioelectron. 50, 239–243.
Tang, D.P., Tang, J., Li, Q.F., Liu, B.Q., Yang, H.H., Chen, G.N., 2011. RSC Adv. 1, 40–43.
Tombelli, S., Minunni, A., Luzi, E., Mascini, M., 2005. Bioelectrochemistry 67, 135–141.
Ueno, Y., Furukawa, K., Matsuo, K., Inoue, S., Hayashi, K., Hibino, H., 2013. Chem. Commun. 49, 10346–10348.
Wang, H., Yang, R., Yang, L., Tan, W., 2009a. ACS Nano 3, 2451–2460.
Wang, J., Munir, A., Li, Z., Zhou, H.S., 2009b. Biosens. Bioelectron. 25, 124–129.
Wang, J., Munir, A., Zhou, H.S., 2009c. Talanta 79, 72–76.
Wang, J., Wang, L.H., Liu, X.F., Liang, Z.Q., Song, S.P., Li, W.X., Li, G.X., Fan, C.H., 2007. Adv. Mater. 19, 3943–3946.
Wang, J., Zhou, H.S., 2008. Anal. Chem. 80, 7174–7178.
Wang, L., Liu, X., Hu, X., Song, S., Fan, C., 2006. Chem. Commun. 36, 3780–3782.
Wang, L., Ma, W., Chen, W., Liu, L., Ma, W., Zhu, Y., Xu, L., Kuang, H., Xu, C., 2011. Biosens. Bioelectron. 26, 3059–3062.
Wang, L., Zhu, C., Han, L., Jin, L., Zhou, M., Dong, S., 2011b. Chem. Commun. 47 (27), 7794–7796.
Wang, W., Chen, C., Qian, M., Zhao, X.S., 2008. Anal. Biochem. 373, 213–219.
Wang, X.Y., Dong, P., He, P.G., Fang, Y.Z., 2010a. Anal. Chim. Acta 658, 128–132.
Wang, Y., Li, Z., Hu, D., Lin, C.T., Li, J., Lin, Y., 2010b. J. Am. Chem. Soc. 132, 9274–9276.
Wang, Y., Tang, L.H., Li, Z.H., Lin, Y.H., Li, J.H., 2014. Nat. Protoc. 9, 1944–1955.
Wang, Y.L., Lee, K., Irudayaraj, J., 2010c. Chem. Commun. 46, 613–615.
Wang, Y.Y., Liu, B., 2009. Langmuir 25, 12787–12793.
Wang, Z., Lu, Y., 2009. J. Mater. Chem. 19, 13.
Wei, H., Li, B., Li, J., Dong, S., Wang, E., 2008. Nanotechnology 19, 095501.
Wood, S.J., 1993. Microchem. J. 47, 330–337.
Wu, C., Yan, L., Wang, C., Lin, H., Wang, C., Chen, X., Yang, C.J., 2010. Biosens. Bioelectron. 25, 2232–2237.
Wu, S.J., Duan, N., Ma, X.Y., Xia, Y., Wang, H.G., Wang, Z.P., Zhang, Q., 2012. Anal. Chem. 84, 6263–6270.
Wu, Z.S., Guo, M.M., Zhang, S.B., Chen, C.R., Jiang, J.H., Shen, G.L., Yu, R.Q., 2007. Anal. Chem. 79, 2933–2939.
Xiang, Y., Tong, A., Lu, Y., 2009. J. Am. Chem. Soc. 131, 15352–15357.
Xiang, Y., Wang, Z., Xing, H., Wong, N.Y., Lu, Y., 2010. Anal. Chem. 82, 4122–4129.
Xiao, Y., Lubin, A.A., Heeger, A.J., Plaxco, K.W., 2005. Angew. Chem. Int. Ed. Engl. 44, 5456–5459.
Xiao, Y., Rowe, A.A., Plaxco, K.W., 2007. J. Am. Chem. Soc. 129, 262–263.
Xu, H., Mao, X., Zeng, Q., Wang, S., Kawde, A.N., Liu, G., 2009a. Anal. Chem. 81, 669–675.
Xu, H., Wang, Y., Huang, X., Li, Y., Zhang, H., Zhong, X., 2012. Analyst 137, 924–931.
Xu, K., Meshik, X., Nichols, B.M., Zakar, E., Dutta, M., Stroscio, M.A., 2014. Nanotechnology 25 (20), 205501.
Xu, Y., Yang, L., Ye, X.Y., He, P.A., Fang, Y.Z., 2006. Electroanalysis 18, 1449–1456.
Xu, Z., Morita, K., Sato, Y., Dai, Q., Nishizawa, S., Teramae, N., 2009b. Chem.

Commun. 42, 6445–6447.
Yamamoto, R., Baba, T., Kumar, P.K., 2000. Genes Cells 5, 389–396.
Yang, L., Fung, C.W., Cho, E.J., Ellington, A.D., 2007. Anal. Chem. 79, 3320–3329.
Yao, G.H., Liang, R.P., Huang, C.F., Zhang, L., Qiu, J.D., 2015a. Anal. Chim. Acta 871, 28–34.
Yao, G.H., Liang, R.P., Yu, X.D., Huang, C.F., Zhang, L., Qiu, J.D., 2015b. Anal. Chem. 87, 929–936.
Yao, J., Sun, Y., Yang, M., Duan, Y.X., 2012. J. Mater. Chem. 22, 14313–14329.
Yi, M., Yang, S., Peng, Z., Liu, C., Li, J., Zhong, W., Yang, R., Tan, W., 2014. Anal. Chem. 86 (7), 3548–3554.
Yu, F.Q., Huang, Y.Z., Cole, A.J., Yang, V.C., 2009. Biomaterials 30, 4716–4722.
Zelada-Guillen, G.A., Bhosale, S.V., Riu, J., Rius, F.X., 2010. Anal. Chem. 82, 9254–9260.
Zelada-Guillen, G.A., Riu, J., Duzgun, A., Rius, F.X., 2009. Angew. Chem. Int. Ed. Engl. 48, 7334–7337.
Zelada-Guillen, G.A., Sebastian-Avila, J.L., Blondeau, P., Riu, J., Rius, F.X., 2012. Biosens. Bioelectron. 31, 226–232.
Zhang, C.Y., Johnson, L.W., 2009. Anal. Chem. 81, 3051–3055.
Zhang, J., Wang, L., Pan, D., Song, S., Boey, F.Y., Zhang, H., Fan, C., 2008a. Small 4, 1196–1200.
Zhang, J., Wang, L.H., Pan, D., Song, S.P., Boey, F.Y.C., Zhang, H., Fan, C.H., 2008b. Small 4, 1196–1200.
Zhang, J., Wang, L.H., Zhang, H., Boey, F., Song, S.P., Fan, C.H., 2010. Small 6, 201–204.
Zhang, S.S., Xia, J.P., Li, X.M., 2008c. Anal. Chem. 80, 8382–8388.
Zhao, H.M., Gao, S., Liu, M., Chang, Y.Y., Fan, X.F., Quan, X., 2013. Microchim. Acta 180, 829–835.
Zhao, J., Chen, G.F., Zhu, L., Li, G.X., 2011. Electrochem. Commun. 13, 31–33.
Zhao, W., Chiuman, W., Brook, M.A., Li, Y., 2007. Chem. Bio. Chem. 8, 727–731.
Zhao, W., Chiuman, W., Lam, J.C., McManus, S.A., Chen, W., Cui, Y., Pelton, R., Brook, M.A., Li, Y., 2008. J. Am. Chem. Soc. 130, 3610–3618.
Zhao, X., Johnson, J.K., 2007. J. Am. Chem. Soc. 129, 10438–10445.
Zhao, X., Tapec-Dytioco, R., Wang, K., Tan, W., 2003. Anal. Chem. 75, 3476–3483.
Zheng, J., Feng, W., Lin, L., Zhang, F., Cheng, G., He, P., Fang, Y., 2007. Biosens. Bioelectron. 23, 341–347.
Zhou, D.J., 2012. Biochem. Soc. Trans. 40, 635–639.
Zhou, L., Ou, L.J., Chu, X., Shen, G.L., Yu, R.Q., 2007. Anal. Chem. 79, 7492–7500.
Zhou, Z.M., Zhou, J., Chen, J., Yu, R.N., Zhang, M.Z., Song, J.T., Zhao, Y.D., 2014. Biosens. Bioelectron. 59, 397–403.
Zhu, Z., Tang, Z., Phillips, J.A., Yang, R., Wang, H., Tan, W., 2008. J. Am. Chem. Soc. 130, 10856–10857.
Zhuang, H.L., Zhen, S.J., Wang, J., Huang, C.Z., 2013. Anal. Methods 5, 208–212.
Zuo, P., Li, X., Dominguez, D.C., Ye, B.C., 2013. Lab Chip 13, 3921–3928.
Zuo, X., Song, S., Zhang, J., Pan, D., Wang, L., Fan, C., 2007. J. Am. Chem. Soc. 129, 1042–1043.